On Distributed Detection in EH-WSNs With Finite-State Markov Channel and Limited Feedback

Ghazaleh Ardeshiri, Azadeh Vosoughi *Senior Member, IEEE* University of Central Florida Email:gh.ardeshiri@knights.ucf.edu, azadeh@ucf.edu

Abstract—We consider a network of N sensors, tasked with solving binary distributed detection, a fusion center (FC), and a feedback channel from the FC to sensors. Each sensor is capable of harvesting energy and is equipped with a finitesize battery to store randomly arrived energy. Sensors process their observations and transmit their symbols to the FC over orthogonal and Markovian time correlated fading channels. The FC fuses the received symbols and makes a global binary decision. We aim at developing adaptive channel-dependent transmit power control policies such that J-divergence based detection metric is maximized at the FC, subject to total transmit power constraint. Modeling quantized fading channel, energy arrival, and battery dynamics as time-homogeneous finite-state Markov chains, and the network lifetime as a geometric random variable, we formulate our power control optimization problem as a discounted infinite-horizon constrained Markov decision process (MDP) problem, where sensors' transmit powers are functions of the battery states, quantized channel gains, and the arrived energies. We utilize stochastic dynamic programming and Lagrangian approach to find the optimal and sub-optimal power control policies. We demonstrate that our sub-optimal policy provides a close-to-optimal performance with a reduced computational complexity and without imposing signaling overhead on sensors.

Index Terms—adaptive channel-dependent power control, channel gain quantization, distributed detection, energy harvesting, J-divergence, finite size battery, geometrically distributed network lifetime, limited feedback, Markov decision process, Markovian time correlated fading model, optimal and suboptimal policies, time-homogeneous finite-state Markov chain.

I. Introduction

Event detection for smarter cities, healthcare systems, farming, and greenhouse environmental monitoring systems is one of the vital tasks in wireless sensor networks (WSNs) [1], [2] and the Internet of things (IoT)-based WSNs [3], [4]. The classical studies of binary distributed detection in [5]–[7] cannot be directly applied to these networks, since the classical works are based on the assumption that the rate-constrained communication channels between distributed sensors and fusion center (FC) are *error-free*. This has motivated researchers to study *channel-dependent* local decision rules for sensors and decision fusion rules for the FC, such that the effect of wireless communication channels in WSNs is integrated into the system designs [8]–[11].

Even for channel-dependent distributed detection system designs, providing a guaranteed detection performance by a conventional WSN, in which sensors are powered by conventional non-rechargeable batteries and become inactive when the stored energy in their batteries is exhausted, is impossible. Although adaptive signal transmission strategies,

including optimal channel-dependent power control [12]–[14] and censoring [15], [16], can enhance the energy efficiency and increase the lifetime of a conventional WSN, they cannot change the fact that the network lifetime is inherently limited. This limited lifetime disrupts the event detection task and drastically degrades the detection performance.

Energy harvesting (EH) from the environment is a promising solution to address the energy constraint problem in conventional WSNs, and to render these networks to self sustainable networks with perpetual lifetimes. The new class of EH-powered WSNs, where nodes have EH capability and are equipped with rechargeable batteries, will be also important for the development of IoT-based WSNs. In EH-powered WSNs power/energy management is necessary, in order to balance the rates of energy harvesting and energy consumption for transmission. If the energy management policy is overly aggressive, sensors may stop functioning, due to energy outage. On the other hand, if the policy is overly conservative, sensors may fail to utilize the excess energy, due to energy overflow, leading into a performance degradation. EH has been also considered in the contexts of data communications [17], [18], cognitive radio systems [19], distributed estimation [20], and distributed detection [21]–[27]. The body of research on EH-enabled communication systems can be grouped into two main categories, depending on the adopted energy arrival model [18], [28]: for deterministic models the transmitter has full knowledge of energy arrival instants and amounts at the beginning of transmission; For stochastic models, suitable for modeling ambient RF and renewable energy sources that are intrinsically time-variant and sporadic, the transmitter only has causal knowledge of energy arrival. In addition, wireless communication channels change randomly in time due to fading. These together prompt the need for developing new power control/energy scheduling strategies for an EH-enabled transmitter that can best exploit and adapt to the random energy arrivals and time-varying fading channels.

Designing power control/energy scheduling schemes corresponding to random energy arrivals and time-varying fading channels can be viewed as a *multistage stochastic optimization problem*, where the goal is to find a sequence of decisions a decision maker has to make, such that a specific metric over a horizon spanning several time slots is optimized (e.g., optimizing transmission completion time, data throughput, outage probability, or symbol error rate in a point-to-point EH-powered wireless communication system [18]). A common approach to solve this sequential decision making problem is to adopt the mathematical framework of Markov decision

processes (MDP). The main ingredients of the MDP are states, actions, rewards, and state transition probabilities. The state could be a composite of states corresponding to fading channel, energy arrival, and battery condition. The action is the transmit power level or the amount of energy to be consumed, and the reward is a function of the states and the actions. The state transition probability describes the transition probability from the current state to the next state with respect to each action. The goal is to find the optimal policy, which specifies the optimal action in the state and maximizes the long-term expected discount infinite-horizon reward starting from the initial state [18].

In the context of distributed detection in WSNs, there are limited works that consider EH-powered sensors [21]–[27]. In the following we provide a concise review of these works, highlight how our present work fills the knowledge gap in the literature, and how it is different from our previous works in [25]–[27].

A. Related Works and Knowledge Gap

Considering a single EH-powered node, that is deployed to monitor the change in its environment, the authors in [21] formulated a quickest change detection problem, where the goal is to detect the time at which the underlying distribution of sensor observation changes. Considering an EH-WSN and choosing deflection coefficient as the detection performance metric, the authors in [24] formulated an adaptive transmit power control strategy based on PHY-MAC cross-layer design. Considering an EH-WSN and choosing error probability as the detection performance metric, the authors in [22] proposed ordered transmission schemes, that can lead to a smaller average number of transmitting sensors, without comprising the detection performance. Modeling the randomly arriving energy units during a time slot as a Bernoulli process, the battery state as a K-state Markov chain, and choosing Bhattacharya distance as the detection performance metric, the authors in [23] have investigated the optimal local decision thresholds at the sensors, such that the detection performance is optimized. We note the system model in [24] lacks a battery to store the harvested energy. Further, the adopted energy arrival model in [24] is deterministic and fading communication channels are orthogonal and independent across transmission blocks. On the other hand, [21], [22] assumed sensor-FC channels are errorfree, and [23] considered the simple Gilbert-Elliot channel model for sensor-FC links (a two-state Markov model). The high level communication channel model, combined with a simple stochastic model for random energy arrival is limiting. Specifically, it does not allow one to study channel-dependent transmit power control strategies. Such a study requires a more realistic communication channel model and stochastic energy arrival model that match the energy needed for a channeldependent transmission. This is the knowledge gap that we address in this work.

To highlight how our present work is different from our previous works in [25]–[27], we briefly summarize them in the following. Modeling the random energy arrival as a Bernoulli process, the dynamics of the battery as a finite-state Markov chain, and considering fading channel model,

in [25] we adopted channel-inversion transmit power control policy, where allocated power is inversely proportional to fading channel state information (CSI) in full precision, and we found the optimal decision thresholds at sensors such that Kullback-Leibler (KL) distance detection metric at the FC is maximized. Different from [25], in [26] we modeled the random energy arrival as an exponential process and assumed that each sensor only knows its quantized CSI and adapts its transmit power according to its battery state and its quantized CSI, such that J-divergence based detection metric at the FC is maximized. Modeling the random energy arrival as a Poisson process in [27], we proposed a novel transmit power control strategy that is parameterized in terms of the channel gain quantization thresholds and the scale factors corresponding to the quantization intervals, and found the jointly optimal quantization thresholds and the scale factors such that Jdivergence based detection metric at the FC is maximized.

Our present work is different from our prior works in [25]-[27] in several aspects. The transmit power control strategies in these works are intrinsically different from our present work, since in [25]–[27] we have assumed that the battery operates at the steady-state and the energy arrival and channel models are independent and identically distributed (i.i.d) across transmission blocks. Consequently, the power optimization problem in [25]–[27] became a deterministic optimization problem, in terms of the optimization variables, and the obtained solutions are different. In this work, the battery is not at the steady-state. Also, both the channel and the energy arrival are modeled as homogeneous finite-state Markov chains (FSMCs). Therefore, the power control optimization problem at hand becomes a multistage stochastic optimization problem, and can be solved via the MDP framework. To the best of our knowledge, this is the first work that develops MDP-based channel-dependent power control policy for distributed detection in EH-WSNs. The MDP framework has been utilized before in [29], [30] to address a quickest change detection problem.

It is worth mentioning that most of the works on EH-enabled wireless communication systems (including single-user and multi-user systems) consider memoryless channel models (e.g., Gaussian MAC [31], [32], AWGN broadcast channel [33], [34], MIMO broadcast and multicast channels [35], [36], Gaussian interference channel [37], orthogonal fading channels where fading process across transmission symbols/blocks is independent [28], [38]–[42]). Markovian channel model allows one to capture the effect of channel memory into the system design and performance (e.g., system throughput, outage probability, paired-wise error probability). Exemplary works of EH-enabled wireless communication systems with Markovian channel model are: [43]–[45], which considered Gilbert-Elliot channel model, and [46]–[51], which considered finite-state Markov channel model.

B. Our Contribution

Given our adopted WSN model (see Fig. 1), we aim at developing an adaptive channel-dependent transmit power control policy for sensors such that a detection performance metric is optimized. We choose the *J*-divergence between

the distributions of the detection statistics at the FC under two hypotheses, as the detection performance metric. Our choice is motivated by the fact that J-divergence is a widely adopted metric for designing distributed detection systems [12], [13], [27], [52]. We note that J-divergence and P_e are related through $P_e > \Pi_0 \Pi_1 e^{-J/2}$, where Π_0, Π_1 are the apriori probabilities of the null and the alternative hypotheses, respectively [12], [13], [52]. Hence, maximizing the Jdivergence is equivalent to minimizing the lower bound on P_e . Modeling the quantized fading channel, the energy arrival, and the dynamics of the battery as homogeneous FSMCs, and the network lifetime as a random variable with geometric distribution, we formulate J-divergence-optimal transmit power control problem, subject to total transmit power constraint, as a discounted infinite-horizon constrained MDP optimization problem, where the control actions (i.e., transmit power levels) are functions of the battery state, quantized CSI, and the arrived energy. We obtain the optimal and sub-optimal policies and propose two algorithms based on value iterations in the MDP. Our main contributions can be summarized as follow:

- Given our adopted system model, we develop the optimal power control policy, using dynamic programming and utilizing the Lagrangian approach to transform the constrained MDP problem into an equivalent unconstrained MDP problem. For the optimal policy, the local action (i.e., a sensor's transmit power) depends on the network state (i.e., all sensors' battery states, quantized CSIs, and the arrived energies), and the computational complexity of the algorithm grows *exponentially* in number of sensors *N*. Implementing this solution requires each sensor to report its battery state and arrived energy to the FC, which imposes a significant signaling overhead to the sensors.
- ullet To eliminate this overhead, we develop a sub-optimal power control policy, using a uniform Lagrangian multiplier to transform the constrained MDP problem into N decoupled unconstrained MDP problems. For the sub-optimal policy, the local action depends on only the local state (i.e., a sensor's battery state, quantized CSI, and the arrived energy), and the computational complexity of the algorithm grows linearly in N. We numerically study the performance of our proposed algorithms and showed that the sub-optimal policy has a close-to-optimal performance.
- We study how our system setup and proposed solutions can be extended to the scenario where sensors are randomly deployed in the field.

C. Paper Organization

The paper organization follows: Section II describes our system and observation models, derives a closed-form expression for the total *J*-divergence and introduces our constrained optimization problem. Section III describes the optimal and the sub-optimal policies. Section IV discusses how our setup can be extended to the scenario where sensors are randomly deployed in the field (i.e., sensors' locations are unknown a-priori). Section V illustrates our numerical results. Section VI concludes our work.

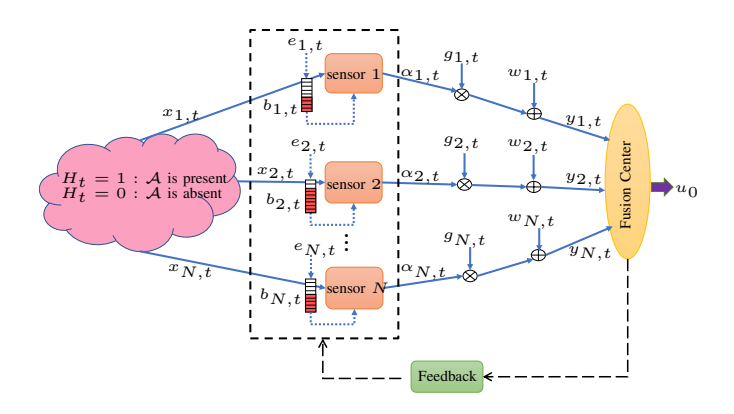


Fig. 1: Our system model and the schematic of battery state in time slot t.

II. SYSTEM MODEL

A. Observation Model at Sensors

We consider a WSN tasked with solving a binary distributed detection problem (see Fig. 1). To describe our signal processing blocks at sensors and the FC as well as energy harvesting model, we divide time horizon into slots of equal length T_s . Each time slot is indexed by an integer t for t = 1, 2, ..., T (see Fig. 2). We model the underlying binary hypothesis H_t in time slot t as a binary random variable $H_t \in \{0,1\}$ with a-priori probabilities $\zeta_0 = \Pr(H_t = 0)$ and $\zeta_1 = \Pr(H_t = 1) = 1 - \zeta_0$. We assume that the hypothesis H_t varies over time slots in an independent and identically distributed (i.i.d.) manner. Let $x_{n,t}$ denote the local observation at sensor n in time slot t. We assume that sensors' observations given each hypothesis with conditional distribution $f(x_{n,t}|H_t=h_t)$ for $h_t \in \{0,1\}$ are independent across sensors. This model is relevant for WSNs that are tasked with detection of a known signal in uncorrelated Gaussian noises with the following signal model

$$H_t = 1: \quad x_{n,t} = \mathcal{A} + v_{n,t},$$

 $H_t = 0: \quad x_{n,t} = v_{n,t}, \text{ for } n = 1, \dots, N,$ (1)

where Gaussian observation noises $v_{n,t} \sim \mathcal{N}(0, \sigma_{v_n}^2)$ are independent over time slots and across sensors. Given observation $x_{n,t}$ sensor n forms local log-likelihood ratio (LLR)

$$\Gamma_n(x_{n,t}) \triangleq \log \left(\frac{f(x_{n,t}|h_t=1)}{f(x_{n,t}|h_t=0)} \right),$$
(2)

and uses its value to choose its non-negative transmission symbol $\alpha_{n,t}$ to be sent to the FC. In particular, when LLR is below a given local threshold θ_n , sensor n does not transmit and let $\alpha_{n,t}=0$. When LLR exceeds the given local threshold θ_n , sensor n chooses $\alpha_{n,t}$ according to the available information (will be explained later). In particular, we have

$$\widehat{\zeta}_{n,0} = \Pr(\alpha_{n,t} = 0) = \zeta_0 (1 - P_{f_n}) + \zeta_1 (1 - P_{d_n}),$$

$$\widehat{\zeta}_{n,1} = \Pr(\alpha_{n,t} \neq 0) = \zeta_0 P_{f_n} + \zeta_1 P_{d_n},$$
(3)

where the false alarm and detection probabilities $P_{\mathbf{f}_n}$ and $P_{\mathbf{d}_n}$ can be determined using our signal model in (1) and given the

Fig. 2: Our adopted time frame structure for harvesting and transmission.

local threshold θ_n

$$P_{f_n} = \Pr(\alpha_{n,t} \neq 0 | h_t = 0) = Q\left(\frac{\theta_n + \mathcal{A}^2 / 2\sigma_{v_n}^2}{\sqrt{\mathcal{A}^2 / \sigma_{v_n}^2}}\right),$$

$$P_{d_n} = \Pr(\alpha_{n,t} \neq 0 | h_t = 1) = Q\left(\frac{\theta_n - \mathcal{A}^2 / 2\sigma_{v_n}^2}{\sqrt{\mathcal{A}^2 / \sigma_{v_n}^2}}\right). \tag{4}$$

Instead of fixing θ_n , one can fix P_{d_n} and let $P_{d_n} = \overline{P}_d, \forall n$. Then the false alarm probability in (4) can be written as $P_{f_n} = Q\left(Q^{-1}(\overline{P}_d) + \sqrt{\mathcal{A}^2/\sigma_{l_n}^2}\right)$.

Note that sensors are typically deployed in hostile outdoor environments (e.g., for forestry fire and volcano monitoring and detection, and battlefield surveillance) in an unattended and distributed manner. Therefore, they are highly susceptible to physical destruction. We include this factor into our modeling by letting $\eta \in [0,1)$ be the probability that a sensor can survive physical destruction or hardware failure and continue to function in time slot t. Defining the network lifetime T as the time until the first sensor fails, we find that T becomes a geometrically distributed random variable with mean $\mathbb{E}\{T\} = 1/(1-\eta)$ [53].

B. Battery State, Energy Harvesting and Transmission Models

We assume sensors are equipped with identical batteries 1 of finite size K cells (units), where each cell corresponds to b_u Joules of stored energy. Therefore, each battery is capable of storing at most Kb_u Joules of harvested energy. Let $b_{n,t} \in \mathcal{B} = \{0,1,...,K\}$ denote the energy state of battery of sensor n at the beginning time slot t (also referred to as the battery state). Note that $b_{n,t} = 0$ and $b_{n,t} = K$ represent energy states of empty battery and full battery, respectively.

Let $e_{n,t}$ be the number of energy units that are harvested and stored at sensor n during time slot t, i.e., at the beginning of time slot t, sensor n knows the value of $e_{n,t-1}$ but not $e_{n,t}$, and hence the harvested energy $e_{n,t}$ cannot be used during slot t. We assume $e_{n,t}$'s are independent across sensors, and model $e_{n,t}$ as a set of independent stationary first-order homogeneous Markov process with transition probability matrix $\Phi_{\mathcal{E}}$. For each time slot t we assume that the random variable $e_{n,t}$ takes values from a finite set $\mathcal{E} = \{E_1, E_2, \dots E_M\}$ where $E_m \in \mathbb{Z}^+$, $E_m < E_{m+1}$. Therefore, matrix $\Phi_{\mathcal{E}}$ is $M \times M$ and its (i,j)-th entry is $[\Phi_{\mathcal{E}}]_{i,j} = \Pr(e_{n,t} = E_i | e_{n,t-1} = E_j)$. This modeling for the harvested energy processes is justified by empirical measurements in the case of solar energy [54].

 1 For the simplicity of notations we assume the batteries are identical. Our system model can be extended to non-identical batteries, where sensor n has a battery of size K_n . Therefore, $\mathcal{B}_n=\{0,1,...,K_n\}$ is the set of battery states, $\mathcal{E}_n=\{E_{1,n},E_{2,n},\ldots E_{M,n}\}$ is the set of harvested energy states, and $\Phi_{\mathcal{E}}^{(n)}$ is the corresponding transition probability matrix. The local state space at sensor n (used in Algorithm 2) is $\mathcal{S}_n=\mathcal{B}_n\times\bar{\mathcal{G}}\times\mathcal{E}_n$, and the global (network) state space (used in Algorithm 1) is $\bar{\mathcal{S}}=\mathcal{S}_1\times\mathcal{S}_2\times\ldots\mathcal{S}_N$. Also, the dimensions of these sets are related through $|\bar{\mathcal{S}}|=\sum_{n=1}^N |\mathcal{S}_n|$. Other than these changes, the remaining analysis is unchanged.

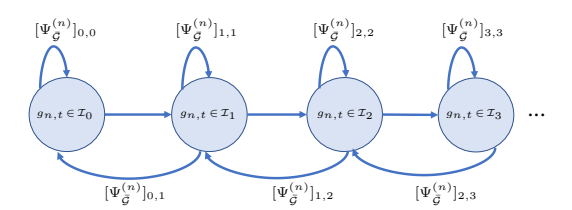


Fig. 3: Our adopted FSMC model for channel fading process.

Let $g_{n,t}$ indicate the narrow-band (flat) fading channel gain between sensor n and the FC during time slot t. We assume $g_{n,t}$'s are independent across sensors. We consider a coherent FC with the knowledge of all channel gains. The FC quantizes $g_{n,t}$ to $\bar{g}_{n,t}$ and informs sensor n of $\bar{g}_{n,t}$, through a bandwidthlimited feedback channel from the FC to sensor n. Suppose the quantizer has L quantization thresholds $\bar{\mathcal{G}} = \{\mu_1, \mu_2, ..., \mu_L\},\$ where $0 = \mu_1 < \mu_2 < ... < \mu_L = \infty$, and $\mathcal{I}_l = [\mu_l, \mu_{l+1}]$ for $l=1,\ldots,L-1$ denote the corresponding quantization intervals. Suppose $\bar{g}_{n,t} = Q(g_{n,t})$ indicates the input-output relationship of the quantizer. If $g_{n,t} \in \mathcal{I}_l$ then $\bar{g}_{n,t} = \mu_l$. We define the probability $\phi_{n,l} = \Pr(\bar{g}_{n,t} = \mu_l)$, which can be found based on the distribution of fading model in terms of the two quantization thresholds μ_l and μ_{l+1} . For Rayleigh fading model, $g_{n,t}^2$ is modeled as an exponential random variable with the mean $\mathbb{E}\{g_{n,t}^2\} = \gamma_{g_n}$ and we have

$$\phi_{n,l} = \Pr(\bar{g}_{n,t} = \mu_l) = e^{\frac{-\mu_l^2}{\gamma_{g_n}}} - e^{\frac{-\mu_{l+1}^2}{\gamma_{g_n}}}.$$
 (5)

We assume $\bar{g}_{n,t}$ is a homogeneous finite-state Markov chain (FSMC) [47] with an $L \times L$ transition probability matrix $\Psi^{(n)}_{\bar{\mathcal{G}}}$ and its (k,l)-th entry is $[\Psi^{(n)}_{\bar{\mathcal{G}}}]_{k,l} = \Pr(\bar{g}_{n,t} = \mu_k | \bar{g}_{n,t-1} = \mu_l)$. Fig. 3 is the schematic representation of this L-state Markov chain. Assuming that the channel fluctuation due to Doppler is slow enough (e.g., slow fading where $f_D T_s \ll 1$ [54]) such that the transition in \bar{g} only happens between adjacent channel states for Rayleigh fading model we have

$$[\Psi_{\bar{\mathcal{G}}}^{(n)}]_{k,l} = \begin{cases} \frac{G(\mu_{l+1}^2)}{\phi_{n,l}}, & k = l+1, \ l = 1, ..., L-1\\ \frac{G(\mu_l^2)}{\phi_{n,l}}, & k = l-1, \ l = 2, ..., L\\ 1 - \frac{G(\mu_l^2) + G(\mu_{l+1}^2)}{\phi_{n,l}}, & k = l, \ l = 2, ..., L-1\\ 1 - \frac{G(\mu_2^2)}{\phi_{n,l}}, & k = 1, \ l = 1\\ 1 - \frac{G(\mu_L^2)}{\phi_{n,L}}, & k = L, \ l = L\\ 0, & \text{O.W.} \end{cases}$$

$$(6)$$

where $G(x) = \sqrt{2\pi x/\gamma_{g_n}} f_D T_s \exp\left(-x/\gamma_{g_n}\right)$ is the number of times that $g_{n,t}$ crosses the level x in a downward direction in T_s seconds, and f_D is the maximum Doppler frequency 2 . We assume the feedback channel from the FC to sensor n has a delay, i.e., at the beginning of time slot t, sensor n only knows $\bar{g}_{n,t-1}$ but not $\bar{g}_{n,t}$.

Let $s_{n,t}$ denote the state of sensor n during time slot t. We characterize $s_{n,t}$ by a three-tuple $s_{n,t} = (b_{n,t}, \bar{g}_{n,t-1}, e_{n,t-1})$.

 2 The choice of fading model affects the expressions of $\phi_{n,l}$ in (5), G(x) in (6), $\hat{J}_{n,t}^{(l)}$ in (30), and $\Omega(x,y)$ in (31). Our problem formulation, analysis, obtained optimal and sub-optimal policies, as well as Algorithms 1 and 2 are valid for other fading models.

We denote the local state space as $\mathcal{S} = \mathcal{B} \times \bar{\mathcal{G}} \times \mathcal{E}$, where \mathcal{B} is the set of battery energy states, $\bar{\mathcal{G}}$ is the set of communication channel states, and \mathcal{E} is the set of energy harvesting states. Let $s_t = (s_{1,t}, s_{2,t}, ..., s_{N,t})$ denote the network state during time slot t and $\bar{\mathcal{S}} = \mathcal{S} \times \mathcal{S} \times ... \mathcal{S}$ denote the network state space, where $\mathcal{S} = \mathcal{B} \times \bar{\mathcal{G}} \times \mathcal{E}$. We refer to $s_{n,t} \in \mathcal{S}$ and $s_t \in \bar{\mathcal{S}}$ as the *local state* and the *global (network) state*, respectively. Clearly, $\mathcal{S}, \bar{\mathcal{S}}$ are discrete and finite. Let the dimensions of $\mathcal{S}, \bar{\mathcal{S}}$ be denoted as $|\mathcal{S}|, |\bar{\mathcal{S}}|$. We have $|\bar{\mathcal{S}}| = |\mathcal{S}|^N = ((K+1)LM)^N$.

In time slot t, if LLR exceeds a given local threshold θ_n , sensor n chooses its non-negative transmission symbol $\alpha_{n,t}$ according to the *available information* (either the local state $s_{n,t}$ or the global state s_t). Note that the amount of energy consumed for transmitting non-negative symbol $\alpha_{n,t}$ cannot be more than the energy stored in the battery, i.e., $\alpha_{n,t}$ must satisfy the inequality $\alpha_{n,t}^2 T_s/b_u \leq b_{n,t}$. This implies that $\alpha_{n,t} \in \mathcal{U}_{n,t}$ where the feasible set $\mathcal{U}_{n,t} = \{0, \sqrt{b_u/T_s}, ..., \sqrt{b_{n,t}b_u/T_s}\}$ is discrete and finite. Let $\alpha_t = (\alpha_{1,t}, \alpha_{2,t}, ..., \alpha_{N,t})$ contain transmission symbols by all sensors. We have $\alpha_t \in \bar{\mathcal{U}}_t = \mathcal{U}_{1,t} \times \mathcal{U}_{2,t} \times ... \mathcal{U}_{N,t}$. Further, we assume that the nodes in the network must satisfy a total transmit power constraint 3 . Such power constraint can be translated into $\sum_{n=1}^N \alpha_{n,t}^2 \leq \mathcal{P}_{tot}$. Our goal is to develop (sub-)optimal adaptive power control strategy such that the detection performance at the FC is optimized.

In Section III we formulate the constrained optimization of transmission symbol $\alpha_{n,t}$ as a discounted infinite-horizon constrained MDP problem. In this problem formulation, $\alpha_{n,t}$ is the action taken by sensor n, and α_t is the collection of actions taken by all sensors, during time slot t. We refer to $\alpha_{n,t}$ as the *local action* and α_t as the *global (network)* action, respectively. We use dynamic programming to solve the problem and provide two types of solutions: (i) the optimal policy, in which local action $\alpha_{n,t}$ depends on the global state $s_t = (s_{1,t}, s_{2,t}, ..., s_{N,t})$ where $s_{n,t} = (b_{n,t}, \bar{g}_{n,t-1}, e_{n,t-1}),$ i.e., during time slot t sensor n has access to the global state s_t and determines its action $\alpha_{n,t}$ according to s_t , and (ii) the sub-optimal policy, in which local action $\alpha_{n,t}$ depends on the local state $s_{n,t}$ only, i.e., during time slot t sensor n has access to the local state $s_{n,t}$ only and determines its action $\alpha_{n,t}$ according to $s_{n,t}$. Let the global state transition probability $\Pr\left(s_{t+1}|s_t,\alpha_t\right)$ denote the probability of entering network state s_{t+1} if network action α_t is taken at network state s_t . Define $b_t = (b_{1,t}, b_{2,t}, ..., b_{N,t}), \ \bar{g}_t = (\bar{g}_{1,t}, \bar{g}_{2,t}, ..., \bar{g}_{N,t}), \ e_t =$ $(e_{1,t},e_{2,t},...,e_{N,t})$. We can simplify the global state transition probability as the product of three conditional probabilities (see Fig. 4)

$$Pr\left(\boldsymbol{s}_{t+1}|\boldsymbol{s}_{t},\boldsymbol{\alpha}_{t}\right)$$

$$=Pr\left(\boldsymbol{b}_{t+1},\bar{\boldsymbol{g}}_{t},\boldsymbol{e}_{t}|\boldsymbol{b}_{t},\bar{\boldsymbol{g}}_{t-1},\boldsymbol{e}_{t-1},\boldsymbol{\alpha}_{t}\right)$$

$$=Pr\left(\boldsymbol{b}_{t+1}|\boldsymbol{b}_{t},\bar{\boldsymbol{g}}_{t},\boldsymbol{e}_{t},\boldsymbol{\alpha}_{t}\right)Pr(\boldsymbol{e}_{t}|\boldsymbol{e}_{t-1})Pr(\bar{\boldsymbol{g}}_{t}|\bar{\boldsymbol{g}}_{t-1}). \tag{7}$$

The second and third conditional probabilities in (7) can

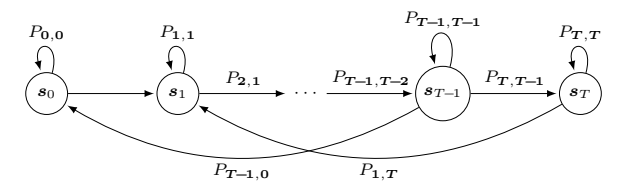


Fig. 4: Schematics of Markov chain corresponding to the global state s_t . In this figure we have $P_{t,t+1} = \Pr\left(s_{t+1} | s_t, \alpha_t\right)$.

be decomposed across sensors, since $\bar{g}_{n,t}$'s and $e_{n,t}$'s are independent across sensors. In other words, we have

$$\Pr(\boldsymbol{e}_t|\boldsymbol{e}_{t-1}) = \prod_{n=1}^{N} \Pr(e_{n,t}|e_{n,t-1}),$$

$$\Pr(\bar{\boldsymbol{g}}_t|\bar{\boldsymbol{g}}_{t-1}) = \prod_{n=1}^{N} \Pr(\bar{g}_{n,t}|\bar{g}_{n,t-1})$$
(8)

in which $\Pr(e_{n,t}|e_{n,t-1}), \Pr(\bar{g}_{n,t}|\bar{g}_{n,t-1})$ are the transition probabilities of $e_{n,t}$ and $\bar{g}_{n,t}$ Markov chains, respectively. To find the first conditional probability in (7), we need to know the dynamic battery state model. The battery state at the beginning of time slot t+1 depends on the battery state at the beginning of time slot t, the harvested energy during time slot t, and the transmission symbol $\alpha_{n,t}$, i.e.,

$$b_{n,t+1} = \min \left\{ [b_{n,t} + e_{n,t} - \alpha_{n,t}^2 T_s / b_u]^+, K \right\},$$
 (9)

where $[x]^+ = \max\{0, x\}.$

Considering the dynamic battery state model in (9) we notice that, conditioned on $e_{n,t}$ and $\alpha_{n,t}$ the value of $b_{n,t+1}$ only depends on the value of $b_{n,t}$ (and not the battery states before time slot t). Hence, the process b_t can be modeled as a Markov chain and the first conditional probability in (7) becomes

$$\Pr\left(\boldsymbol{b}_{t+1}|\boldsymbol{b}_{t},\bar{\boldsymbol{g}}_{t},\boldsymbol{e}_{t},\boldsymbol{\alpha}_{t}\right) = \begin{cases} 1 & \text{if (9) is satisfied } \forall n \\ 0 & \text{otherwise,} \end{cases}$$
(10)

We define the reward function in Section II-D.

C. Received Signals at FC and Optimal Bayesian Fusion Rule

In each time slot, sensors send their data symbols to the FC over orthogonal fading channels. The received signal at the FC from sensor n corresponding to time slot t is

$$y_{n,t} = g_{n,t} \alpha_{n,t} + w_{n,t}, \quad \text{for } n = 1, \dots, N$$
 (11)

where $w_{n,t} \sim \mathcal{N}(0, \sigma_{w_n}^2)$ is the additive Gaussian noise. We assume $w_{n,t}$'s are i.i.d. over time slots and independent across sensors. Let $\boldsymbol{y}_t = [y_{1,t}, y_{2,t}, \dots, y_{N,t}]$ denote the vector that includes the received signals at the FC from all sensors in time slot t. The FC applies the optimal Bayesian fusion rule $\Gamma_0(.)$ to the received vector \boldsymbol{y}_t and obtains a global decision $u_{0,t} = \Gamma_0(\boldsymbol{y}_t)$, where $u_{0,t} \in \{0,1\}$. In particular, we have

$$u_{0,t} = \Gamma_0(\boldsymbol{y}_t) = \begin{cases} 1, & \Delta_t > \tau, \\ 0, & \Delta_t < \tau, \end{cases}$$
(12)

³ This is a common assumption in the WSN literature [55], [56]. From practical perspectives having such a constraint is meaningful, since (i) it enhances the network energy efficiency, (ii) it allows us to fairly compare performance of networks with different sizes (given the same transmission resources), and (iii) it limits the interference power imposed on the neighboring WSNs.

where the decision threshold is $\tau = \log(\frac{\zeta_0}{\zeta_1})$ and

$$\Delta_t = \log \left(\frac{f(\boldsymbol{y}_t | h_t = 1)}{f(\boldsymbol{y}_t | h_t = 0)} \right), \tag{13}$$

and $f(\boldsymbol{y}_t|h_t)$ is the conditional probability density function (pdf) of the received vector \boldsymbol{y}_t at the FC. From Bayesian perspective, the natural choice to measure the detection performance corresponding to the global decision $u_{0,t}$ at the FC is the error probability, defined as

$$P_e = \zeta_0 \Pr(u_{0,t} = 1 | h_t = 0) + \zeta_1 \Pr(u_{0,t} = 0 | h_t = 1)$$

= $\zeta_0 \Pr(\Delta_t > \tau | h_t = 0) + \zeta_1 \Pr(\Delta_t < \tau | h_t = 1).$ (14)

However, finding a closed form expression for P_e is mathematically intractable. Instead, we choose the total J-divergence between the distributions of the detection statistics at the FC under different hypotheses, as our detection performance metric. This choice allows us to provide a tractable analysis. Next, we define the total J-divergence and derive a closed-form expression for it, using Gaussian approximation.

D. Total J-Divergence Derivation and Reward Function

Consider two pdfs of a continuous random variable x, denoted as $\eta_1(x)$ and $\eta_2(x)$. By definition [12], the J-divergence between $\eta_1(x)$ and $\eta_0(x)$, denoted as $J(\eta_1,\eta_0)$, is $J(\eta_1,\eta_0)=D(\eta_1||\eta_0)+D(\eta_0||\eta_1)$, where $D(\eta_i||\eta_j)$ is the non-symmetric Kullback-Leibler (KL) distance between $\eta_i(x)$ and $\eta_j(x)$. The KL distance $D(\eta_i||\eta_j)$ is defined as

$$D(\eta_i||\eta_j) = \int_{-\infty}^{\infty} \log\left(\frac{\eta_i(x)}{\eta_j(x)}\right) \eta_i(x) dx.$$
 (15)

Therefore, we obtain

$$J(\eta_1, \eta_0) = \int_{-\infty}^{\infty} \left[\eta_1(x) - \eta_0(x) \right] \log \left(\frac{\eta_1(x)}{\eta_0(x)} \right) dx. \quad (16)$$

In our problem setup, the two conditional pdfs $f(\boldsymbol{y}_t|h_t=1)$ and $f(\boldsymbol{y}_t|h_t=0)$ in (13) play the role of $\eta_1(x)$ and $\eta_0(x)$, respectively. Let $J_{tot,t}$ denote the J-divergence between $f(\boldsymbol{y}_t|h_t=1)$ and $f(\boldsymbol{y}_t|h_t=0)$. The pdf of vector \boldsymbol{y}_t given h_t is

$$f(\mathbf{y}_t|h_t) = \prod_{n=1}^{N} f(y_{n,t}|h_t)$$
 for $h_t = 0, 1.$ (17)

where the equality in (17) holds since the received signals from sensors at the FC, given h_t , are conditionally independent. Let $J_{n,t}$ represent the J-divergence between the two conditional pdfs $f(y_{n,t}|h_t=1)$ and $f(y_{n,t}|h_t=0)$. We have

$$\begin{split} J_{n,t} &= \\ &\int_{-\infty}^{\infty} \! \left[\! f(y_{n,t}|h_t \!=\! 1) \! - \! f(y_{n,t}|h_t \!=\! 0) \! \right] \! \log \! \left(\! \frac{\! f(y_{n,t}|h_t \!=\! 1)}{\! f(y_{n,t}|h_t \!=\! 0)} \! \right) \! dy_{n,t}. \end{split} \tag{18}$$

Based on (17), the total J-divergence, denoted as $J_{tot,t}$, is $J_{tot,t} = \sum_{n=1}^{N} J_{n,t}$. Note that $f(y_{n,t}|h_t=0) = f(y_{n,t}|\alpha_{n,t} \neq 0)P_{\mathrm{f}_n} + f(y_{n,t}|\alpha_{n,t}=0)(1-P_{\mathrm{f}_n})$ and $f(y_{n,t}|h_t=1) = f(y_{n,t}|\alpha_{n,t}\neq 0)P_{\mathrm{d}_n} + f(y_{n,t}|\alpha_{n,t}=0)(1-P_{\mathrm{d}_n})$ are Gaussian mixtures and the J-divergence between two Gaussian mixture

densities does not have a closed-form expression [12], [27]. We approximate $J_{n,t}$ in (18) using the Gaussian densities $f^G(y_{n,t}|h_t) \sim \mathcal{N}(m_{n,h},\Upsilon^2_{n,h})$, where $m_{n,h}$ and $\Upsilon^2_{n,h}$ are obtained from matching the first and second order moments of the actual and the approximate distributions. For our problem setup, $m_{n,h}$ and $\Upsilon^2_{n,h}$ are

$$\begin{split} m_{n,0} &= g_{n,t} \alpha_{n,t} P_{\mathbf{f}_n}, \quad \Upsilon_{n,0}^2 = g_{n,t}^2 \alpha_{n,t}^2 P_{\mathbf{f}_n} (1 - P_{\mathbf{f}_n}) + \sigma_{w_n}^2, \\ m_{n,1} &= g_{n,t} \alpha_{n,t} P_{\mathbf{d}_n}, \quad \Upsilon_{n,1}^2 = g_{n,t}^2 \alpha_{n,t}^2 P_{\mathbf{d}_n} (1 - P_{\mathbf{d}_n}) + \sigma_{w_n}^2. \end{split}$$

The *J*-divergence between two Gaussian densities, represented as $J(f^G(y_{n,t}|h_t=1), f^G(y_{n,t}|h_t=0))$, in terms of their means and variances is [12], [27]

$$J(f^{G}(y_{n}|h=1), f^{G}(y_{n}|h=0)) = \frac{\Upsilon_{n,1}^{2} + (m_{n,1} - m_{n,0})^{2}}{\Upsilon_{n,0}^{2}} + \frac{\Upsilon_{n,0}^{2} + (m_{n,0} - m_{n,1})^{2}}{\Upsilon_{n,1}^{2}}.$$
(20)

Substituting $m_{n,h}$ and $\Upsilon^2_{n,h}$ of (19) into (20) we approximate $J_{n,t}$ in (18) as the following

$$J_{n,t}(g_{n,t},\alpha_{n,t}) = \frac{\sigma_{w_n}^2 + A_n g_{n,t}^2 \alpha_{n,t}^2}{\sigma_{w_n}^2 + B_n g_{n,t}^2 \alpha_{n,t}^2} + \frac{\sigma_{w_n}^2 + C_n g_{n,t}^2 \alpha_{n,t}^2}{\sigma_{w_n}^2 + D_n g_{n,t}^2 \alpha_{n,t}^2},$$
(21)

where

$$A_{n} = P_{f_{n}}(1 - P_{d_{n}}) + P_{d_{n}}(P_{d_{n}} - P_{f_{n}}),$$

$$C_{n} = P_{d_{n}}(1 - P_{f_{n}}) - P_{f_{n}}(P_{d_{n}} - P_{f_{n}}),$$

$$B_{n} = P_{d_{n}}(1 - P_{d_{n}}), \quad D_{n} = P_{f_{n}}(1 - P_{f_{n}}).$$
(22)

The notation $J_{n,t}(g_{n,t},\alpha_{n,t})$ in (21) is to emphasize that Jdivergence depends on both transmission symbol $\alpha_{n,t}$ and fading channel gain $g_{n,t}$. The dependency on $g_{n,t}$ stems from the fact that the FC has full knowledge of all channel gains $g_{n,t}$'s, and the optimal Bayesian fusion rule utilizes this full information to make the binary decision. On the other hand, sensor n only knows $\bar{g}_{n,t-1} = Q(g_{n,t-1})$. Hence, $\alpha_{n,t}$ can only depend on $\bar{g}_{n,t-1}$. To resolve this issue, we take the average of $J_{n,t}$ over $g_{n,t}$, conditioned on $\bar{g}_{n,t-1}$. Let $\mathbb{E}_{g_{n,t}|\bar{g}_{n,t-1}}\{J_{n,t}(g_{n,t},\alpha_{n,t})|\bar{g}_{n,t-1}\}$ denote the average of Jdivergence over $g_{n,t}$ when action $\alpha_{n,t}$ is taken according to the available information at sensor n, conditioned on $\bar{g}_{n,t-1}$. Let $r(\alpha_{n,t})$ indicate the immediate reward function of sensor n at time slot t. We define the immediate reward function of sensor n as the average of J-divergence over $g_{n,t}$ when action $\alpha_{n,t} \neq 0$ is taken according to the available information at sensor n, conditioned on $\bar{q}_{n,t-1}$, i.e.,

$$r(\alpha_{n,t}) = \widehat{\zeta}_{n,1} \mathbb{E}_{g_{n,t}|\bar{g}_{n,t-1}} \{ J(g_{n,t}, \alpha_{n,t}) | \bar{g}_{n,t-1} \}$$
 (23)

where $\widehat{\zeta}_{n,1}=\Pr(\alpha_{n,t}\neq 0)$ is given in (3). Note that when action $\alpha_{n,t}=0$ is taken from (21) we find $J_{n,t}(g_{n,t},0)=2$. By defining the immediate reward as (23) we neglect the constant term $\widehat{\zeta}_{n,0}\mathbb{E}_{g_{n,t}|\overline{g}_{n,t-1}}\{J(g_{n,t},0)|\overline{g}_{n,t-1}\}=2\widehat{\zeta}_{n,0}$ and do not count it toward the immediate reward function. To compute the immediate reward function in (23), first we define the

following

$$\hat{J}_{n,t}^{(l)} = \mathbb{E}_{g_{n,t}|\bar{g}_{n,t}=\mu_l} \{ J_{n,t} (g_{n,t}, \alpha_{n,t}) | \bar{g}_{n,t} = \mu_l \}
\bar{J}_{n,t}^{(l)} = \mathbb{E}_{g_{n,t}|\bar{g}_{n,t-1}=\mu_l} \{ J_{n,t} (g_{n,t}, \alpha_{n,t}) | \bar{g}_{n,t-1} = \mu_l \}$$
(24)

Hence, the immediate reward function in (23) can be rewritten in terms of $\bar{J}_{n,t}^{(l)}$ for l=1,...,L as

$$r(\alpha_{n,t}) = \widehat{\zeta}_{n,1} \left(\sum_{l=2}^{L-1} \underbrace{\Pr(\bar{g}_{n,t-1} = \mu_l)}_{=\phi_{n,l}} \bar{J}_{n,t}^{(l)} + \underbrace{\Pr(\bar{g}_{n,t-1} = \mu_l)}_{=\phi_{n,1}} \bar{J}_{n,t}^{(1)} + \underbrace{\Pr(\bar{g}_{n,t-1} = \mu_L)}_{=\phi_{n,L}} \bar{J}_{n,t}^{(L)} \right) (25)$$

To fully characterize the reward function in (25) we need to find $\bar{J}_{n,t}^{(l)}$ defined in (24) for l=1,...,L. When $\bar{g}_{n,t-1}=\mu_l$ for l=2,...,L-1, from (6) we have

$$\bar{g}_{n,t} = \begin{cases} \mu_{l-1} & \text{with probability } [\Psi_{\bar{\mathcal{G}}}^{(n)}]_{l-1,l} \\ \mu_{l} & \text{with probability } [\Psi_{\bar{\mathcal{G}}}^{(n)}]_{l,l} \\ \mu_{l+1} & \text{with probability } [\Psi_{\bar{\mathcal{G}}}^{(n)}]_{l+1,l} \end{cases}$$

$$(26)$$

When $\bar{g}_{n,t-1} = \mu_1$, from (6) we have

$$\bar{g}_{n,t} = \begin{cases} \mu_1 & \text{with probability } [\Psi_{\bar{\mathcal{G}}}^{(n)}]_{1,1} \\ \mu_2 & \text{with probability } [\Psi_{\bar{\mathcal{G}}}^{(n)}]_{2,1} \end{cases}$$
 (27)

and when $\bar{g}_{n,t-1} = \mu_L$, from (6) we have

$$\bar{g}_{n,t} = \begin{cases} \mu_{L-1} & \text{with probability } [\Psi_{\bar{\mathcal{G}}}^{(n)}]_{L-1,L} \\ \mu_{L} & \text{with probability } [\Psi_{\bar{\mathcal{G}}}^{(n)}]_{L,L-1} \end{cases}$$
 (28)

Therefore, $\bar{J}_{n,t}^{(l)}$ and $\hat{J}_{n,t}^{(l)}$ in (24) become related as the following

$$\bar{J}_{n,t}^{(l)} = \begin{cases} [\Psi_{\vec{G}}^{(n)}]_{l-1,l} \hat{J}_{n,t}^{(l-1)} + [\Psi_{\vec{G}}^{(n)}]_{l,l} \hat{J}_{n,t}^{(l)} + [\Psi_{\vec{G}}^{(n)}]_{l+1,l} \hat{J}_{n,t}^{(l+1)} \ l \neq 1, L \\ [\Psi_{\vec{G}}^{(n)}]_{1,1} \hat{J}_{n,t}^{(1)} + [\Psi_{\vec{G}}^{(n)}]_{2,1} \hat{J}_{n,t}^{(2)} \ l = 1 \\ [\Psi_{\vec{G}}^{(n)}]_{L-1,L} \hat{J}_{n,t}^{(L-1)} + [\Psi_{\vec{G}}^{(n)}]_{L,L} \hat{J}_{n,t}^{(L)} \ l = L \end{cases}$$

$$(29)$$

Note that $\hat{J}_{n,t}^{(l)}$ in (24) can be obtained based on the distribution of fading model. For Rayleigh fading model, we have [27]

$$\hat{J}_{n,t}^{(l)} = \phi_{n,l} \left[\Omega(\alpha_{n,t}^2, \mu_{l+1}^2) - \Omega(\alpha_{n,t}^2, \mu_l^2) \right], \tag{30}$$

where the two dimensional function $\Omega(x,y)$ in (30) is

$$\Omega(x,y) \triangleq \frac{1}{B_{n}x} \left[\sigma_{w_{n}}^{2} \beta_{1}(x,y) - \frac{A_{n}}{B_{n}} \sigma_{w_{n}}^{2} \beta_{1}(x,y) - A_{n}x e^{(-y\gamma_{g_{n}})} \right] + \frac{1}{D_{n}x} \left[\sigma_{w_{n}}^{2} \beta_{2}(x,y) - \frac{C_{n}}{D_{n}} \sigma_{w_{n}}^{2} \beta_{2}(x,y) - C_{n}x e^{(-y\gamma_{g_{n}})} \right], \tag{31}$$

Also, A_n , B_n , C_n and D_n are given in (22) and the two dimensional functions $\beta_1(x,y)$ and $\beta_2(x,y)$ in (31) are

$$\beta_1(x,y) \triangleq \gamma_{g_n} \exp\left(\frac{\sigma_{w_n}^2 \gamma_{g_n}}{x B_n}\right) \operatorname{Ei}\left(-\gamma_{g_n} y - \frac{\sigma_{w_n}^2 \gamma_{g_n}}{x B_n}\right),$$

$$\beta_2(x,y) \triangleq \gamma_{g_n} \mathrm{exp}\Big(\frac{\sigma_{w_n}^2 \gamma_{g_n}}{x D_n}\Big) \mathrm{Ei}\Big(-\gamma_{g_n} y - \frac{\sigma_{w_n}^2 \gamma_{g_n}}{x D_n}\Big).$$

In summary, the reward function in (25) can be written as

$$r(\alpha_{n,t}) = \widehat{\zeta}_{n,1} \left(\sum_{l=2}^{L-1} \phi_{n,l} \bar{J}_{n,t}^{(l)} + \phi_{n,1} \bar{J}_{n,t}^{(1)} + \phi_{n,L} \bar{J}_{n,t}^{(L)} \right)$$
(32)

in which $\bar{J}_{n,t}^{(l)}$ is given in (29). The immediate network reward function at time slot t, denoted as $r(\alpha_t)$, is the sum of the reward functions of all sensors

$$r(\boldsymbol{\alpha}_t) = \sum_{n=1}^{N} r(\alpha_{n,t}). \tag{33}$$

where $r(\alpha_{n,t})$ is given in (32).

At every time slot t, sensor n decides the transmission symbol $\alpha_{n,t}$ according to the available information (either the local state $s_{n,t}$ or the global state s_t) such that the discounted sum of reward is maximized, subject to two constraints: (i) the amount of energy consumed for transmission symbol $\alpha_{n,t}$ cannot be more than the energy stored in the battery $b_{n,t}$, i.e., $\alpha_{n,t}^2 T_s/b_u \leq b_{n,t}$, or equivalently, $\alpha_{n,t} \in \mathcal{U}_{n,t}$, $\forall n,t$, (ii) the nodes in the network must satisfy a total transmit power constraint, i.e., $\sum_{n=1}^N \alpha_{n,t}^2 \leq \mathcal{P}_{tot}$, $\forall t$.

In the next section we formulate the constrained optimization of $\alpha_{n,t}$ as a discounted infinite-horizon constrained MDP problem. We use dynamic programming to solve the problem and provide two types of solutions: (i) the optimal policy, in which the local action $\alpha_{n,t}$ depends on the global state s_t , and (ii) the sub-optimal policy, in which the local action $\alpha_{n,t}$ depends on the local state $s_{n,t}$ only.

III. PROBLEM FORMULATION

We start our problem formulation by defining the set of feasible policies. Let δ_t denote a general decision rule that describes how a network action α_t is selected according to the global state s_t in time slot t, i.e., $\alpha_t = \delta_t(s_t)$, and $\pi = (\delta_1, \delta_2, ... \delta_T)$ be the corresponding policy for t = 1, ..., T, i.e., π is the sequence of decision rules to be employed for time slots t = 1, ..., T [57, pp.21]. We say that a policy π is feasible if it satisfies the two constraints: (i) $\alpha_t \in \overline{\mathcal{U}}_t$, $\forall t$, (ii) $\sum_{n=1}^N \alpha_{n,t}^2 \leq \mathcal{P}_{tot}$, $\forall t$. Let Π be the set of feasible policies π . Then, for any given global state s_1 at the first time slot t = 1, the expected network reward between the first time slot until a sensor stops functioning with policy $\pi \in \Pi$ is given by

$$V_{\pi}(\mathbf{s}_{1}) = \mathbb{E}\left\{\mathbb{E}_{T}\left\{\sum_{t=1}^{T} r(\boldsymbol{\alpha}_{t})\right\} \middle| \mathbf{s}_{1}, \pi\right\}$$
s.t. $\boldsymbol{\alpha}_{t} \in \bar{\mathcal{U}}_{t}, \sum_{n=1}^{N} \alpha_{n,t}^{2} \leq \mathcal{P}_{tot}, \ \forall t$ (34)

where the outer expectation $\mathbb{E}\{.\}$ in (34) denotes the statistical expectation taken over all relevant random variables given initial global state s_1 and policy π . The inner expectation $\mathbb{E}_T\{.\}$ in (34) denotes the expectation with respect to the random variable T. Note that with a different initial global state s_1 and a different policy π , a different network action α_t will be selected in time slot t, which results in a different state transition probability $\Pr\left(s_{t+1}|s_t,\alpha_t\right)$ when the outer expectation $\mathbb{E}\{.\}$ in (34) is computed. Since T is a geometric

random variable with mean $\mathbb{E}\{T\} = 1/(1-\eta)$, (34) is equivalent to the objective function of an infinite-horizon MDP with discounted reward given by [57, Proposition 5.3.1]

$$V_{\pi}(\boldsymbol{s}_{1}) = \mathbb{E}\left\{\sum_{t=1}^{\infty} \eta^{t} r(\boldsymbol{\alpha}_{t}) | \boldsymbol{s}_{1}, \pi\right\}$$
s.t. $\boldsymbol{\alpha}_{t} \in \bar{\mathcal{U}}_{t}, \sum_{n=1}^{N} \alpha_{n,t}^{2} \leq \mathcal{P}_{tot}, \forall t$ (35)

where η in (35) can be interpreted as the discount factor of the model and $V_{\pi}(s_1)$ in (35) can be interpreted as the long-term expected network reward starting from an initial global state s_1 and continuing with the policy π from then on [57]. Since the network will stop functioning at some time in the future, the network reward at time slot t is discounted by factor η^t . The problem in (35) is our discounted infinite-horizon constrained MDP problem.

One can easily show that the objective function $V_{\pi}(s_1)$ in (35) converges to a finite value [57, pp. 121]. The proof follows. First, we note

$$\sup_{\mathbf{s}_t \in \bar{\mathcal{S}}, \ \mathbf{\alpha}_t \in \bar{\mathcal{U}}_t} |r(\mathbf{\alpha}_t)| \le \sup_{\mathbf{s}_t \in \bar{\mathcal{S}}, \ \mathbf{\alpha}_t \in \bar{\mathcal{U}}_t} \sum_{n=1}^N |r(\alpha_{n,t})|$$
(36)

Next, we examine $r(\alpha_{n,t})$ in (32) and we note that $\widehat{\zeta}_{n,1}, \{\phi_{n,l}\}_{l=1}^L$ are probabilities and $\{\bar{J}_{n,t}^{(l)}\}_{l=1}^L$ depend on the two dimensional $\Omega(.,.), \beta_1(.,.), \beta_2(.,.)$ functions, which all take finite values $\forall s_t \in \bar{\mathcal{S}}, \ \alpha_t \in \bar{\mathcal{U}}_t$. Hence the right-hand side of (36) is finite. This completes the proof. Due to Markovian property of MDP problems, it suffices to consider only $\mathit{Markovian policies}$. Hence, our aim is finding the optimal Markovian policy $\pi \in \Pi$ that maximizes $V_\pi(s_1)$ in (35). That is, given the initial global state s_1 , our goal is to obtain the optimal expected total discounted network reward $V^*(s_1)$ and the optimal Markovian policy $\pi^* \in \Pi$ defined as follows:

$$V^*(\boldsymbol{s}_1) = \max_{\pi \in \Pi} V_{\pi}(\boldsymbol{s}_1), \quad \pi^* = \arg \max_{\pi \in \Pi} V_{\pi}(\boldsymbol{s}_1)$$
s.t. $\boldsymbol{\alpha}_t \in \bar{\mathcal{U}}_t, \quad \sum_{n=1}^N \alpha_{n,t}^2 \le \mathcal{P}_{tot}, \quad \forall t$ (37)

A Markovian policy $\pi = (\delta_1, \delta_2, ... \delta_T)$ is said to be stationary deterministic if $\delta_t = \delta$ for all time slots such that $\pi = (\delta, \delta, ..., \delta)$ and δ is deterministic [57, pp. 21]. The existence of a stationary deterministic optimal policy is guaranteed when the network state space \bar{S} is discrete and finite [57]. Thus, our objective is to find the optimal stationary deterministic policy $\pi \in \Pi$ that maximizes $V_{\pi}(s_1)$ in (35).

A. Finding the Optimal Policy

To maximize $V_{\pi}(s_1)$ in (35), we first utilize the Lagrangian approach [58], [59] to transform the constrained MDP optimization problem into an equivalent unconstrained MDP optimization problem. For each global state s_t we introduce a Lagrangian multiplier λ_{s_t} associated with the constraint

 $\left(\sum_{n=1}^{N} \alpha_{n,t}^2 - \mathcal{P}_{tot}\right)$. We define the Lagrangian value function $\mathcal{L}(s_t, \lambda_{s_t})$ using the dynamic programming [59]

$$\mathcal{L}(\boldsymbol{s}_{t}, \lambda_{\boldsymbol{s}_{t}}) = \max_{\pi \in \Pi} \left\{ \underbrace{L(\boldsymbol{s}_{t}, \boldsymbol{\alpha}_{t}, \lambda_{\boldsymbol{s}_{t}})}_{= \text{ term } 1} + \underbrace{\eta \sum_{\boldsymbol{s}_{t+1}} \Pr\left(\boldsymbol{s}_{t+1} | \boldsymbol{s}_{t}, \boldsymbol{\alpha}_{t}\right) \mathcal{L}(\boldsymbol{s}_{t+1}, \lambda_{\boldsymbol{s}_{t+1}})}_{= \text{ term } 2} \right\}, \tag{38}$$

where $L(s_t, \alpha_t, \lambda_{s_t})$ is defined as

$$L(s_t, \alpha_t, \lambda_{s_t}) = r(\alpha_t) - \lambda_{s_t} \left(\sum_{n=1}^{N} \alpha_{n,t}^2 - \mathcal{P}_{tot} \right).$$
 (39)

In fact, $L(s_t, \alpha_t, \lambda_{s_t})$ in (39) can be interpreted as the modified network reward function at time slot t, where the cost of violating the constraint is subtracted from the immediate reward $r(\alpha_t)$ earned in time slot t. On the other hand, term 2 in $\mathcal{L}(s_t, \lambda_{s_t})$ is the expected total discounted future network reward if network action α_t is chosen. Since α_t can be zero or non-zero, term 2 can be expanded as (40). Note that $\alpha_t = 0$ only if $\alpha_{n,t} = 0, \forall n$, i.e., when LLR is below the local threshold $\theta_n, \forall n$. Using (3) we find $\Pr(\alpha_t = 0) = \prod_{n=1}^N \Pr(\alpha_{n,t} = 0) = \prod_{n=1}^N \widehat{\zeta}_{n,0}$ and $\Pr(\alpha_t \neq 0) = 1 - \Pr(\alpha_t = 0)$.

With fixed λ_{s_t} , the constrained MDP problem in (35) can be viewed as an unconstrained MDP problem in (40) with the modified network reward function $L(s_t, \alpha_t, \lambda_{s_t})$ at time slot t given in (39). Let $U(\lambda_{s_t})$ denote the Lagrangian dual function, where

$$U(\lambda_{s_t}) = \max_{s} \mathcal{L}(s_t, \lambda_{s_t})$$
 (41)

Then the Lagrangian dual problem can be written as

$$\min_{\lambda_{\boldsymbol{s}_t} \ge 0} U(\lambda_{\boldsymbol{s}_t}) \tag{42}$$

The resulting dual solution has zero duality gap compared to the primary problem in (38) [59, pp.2]. To solve the dual problem in (42), we iteratively solve the following two sub-problems until a pre-specified convergence criterion is reached. The outer minimization sub-problem (the outer loop in Algorithm 1 with iteration index i) updates $\lambda_{s_t}^i$. The inner maximization sub-problem (the inner loop in Algorithm 1 with iteration index j) finds the optimal π_i given $\lambda_{s_t}^i$. The pseudo code of the algorithm is given in Algorithm 1.

- 1) the inner maximization sub-problem: Given $\lambda_{s_t}^i$ we adopt the value iteration algorithm [60] to find the optimal policy π_i . The convergence criterion is $|\mathcal{L}^j(s_t, \lambda_{s_t}^i) \mathcal{L}^{j-1}(s_t, \lambda_{s_t}^i)| < \epsilon_1(1-\eta)/2\eta$, for a given ϵ_1 , where $\mathcal{L}^j(s_t, \lambda_{s_t}^i)$ indicates the long-term expected reward in the j-th iteration from (40).
- 2) the outer minimization sub-problem: The outer minimization over the Lagrangian multiplier λ_{s_t} is a linear programming problem.

We use the sub-gradient method to update $\lambda_{s_t}^i$ as the following.

$$\lambda_{\mathbf{s}_t}^{i+1} = \left[\lambda_{\mathbf{s}_t}^i + \beta^i \left(\sum_{n=1}^N \alpha_{n,t}^2 - \mathcal{P}_{tot}\right)\right]^+, \quad (43)$$

$$\mathcal{L}(\boldsymbol{s}_{t}, \lambda_{\boldsymbol{s}_{t}}) = \max_{\boldsymbol{\pi} \in \Pi} \left\{ \underbrace{L(\boldsymbol{s}_{t}, \boldsymbol{\alpha}_{t}, \lambda_{\boldsymbol{s}_{t}})}_{= \text{ term } 1} + \eta \left(\Pr(\boldsymbol{\alpha}_{t} = 0) \sum_{\boldsymbol{s}_{t+1}} \Pr(\boldsymbol{s}_{t+1} | \boldsymbol{s}_{t}, 0) \mathcal{L}(\boldsymbol{s}_{t+1}, \lambda_{\boldsymbol{s}_{t+1}}) + \Pr(\boldsymbol{\alpha}_{t} \neq 0) \sum_{\boldsymbol{s}_{t+1}} \Pr(\boldsymbol{s}_{t+1} | \boldsymbol{s}_{t}, \boldsymbol{\alpha}_{t}) \mathcal{L}(\boldsymbol{s}_{t+1}, \lambda_{\boldsymbol{s}_{t+1}}) \right) \right\}.$$
(40)

Algorithm 1: optimal power control algorithm Inputs: $\bar{\mathcal{S}}, \Phi_{\mathcal{E}}, \Psi^{(n)}_{\bar{\mathcal{G}}}, K, \gamma_{g_n}, \sigma^2_{w_n}, \mathcal{P}_{tot}, P_{\mathbf{f}_n}, P_{\mathbf{d}_n}, \eta, \epsilon_1, \epsilon_2$ Output: optimal policy π

```
1: Specify \epsilon_1 > 0, \epsilon_2 > 0 set \mathcal{L}(s_1, \lambda_{s_1}) = 0, s_t \in \bar{\mathcal{S}} set i = 1;

2: for fixed \lambda_{s_t}^i do

3: Set j = 1, for each s_t \in \bar{\mathcal{S}} do

| for each \alpha_t \in \mathcal{U}_{s_t} do
| calculate
| \mathcal{F}(s_t, \alpha_t, \lambda_{s_t}^i) = L(s_t, \alpha_t, \lambda_{s_t}^i) + \eta \sum_{s_{t+1}} \Pr\left(s_{t+1} | s_t, \alpha_t\right) \mathcal{L}^{j-1}(s_{t+1}, \lambda_{s_{t+1}}^i)
| end
| calculate \mathcal{L}^j(s_t, \lambda_{s_t}^i) = \max_{\pi_i \in \Pi} \{\mathcal{F}(s_t, \alpha_t, \lambda_{s_t}^i)\};
| end
| 4: If \max_{s_t \in \mathcal{S}} |\mathcal{L}^j(s_t, \lambda_{s_t}^i) - \mathcal{L}^{j-1}(s_t, \lambda_{s_t}^i)| < \epsilon_1 (1 - \eta)/2\eta, go to Step 5. Otherwise, increase j and go back to Step 3.

5: We obtain the optimal policy

\pi_i^* = \arg\max_{\pi \in \Pi} \left\{ \mathcal{L}^j(s_t, \lambda_{s_t}^i) \right\}.
```

end

6: Update $\lambda_{s_t}^i$ using the rule in (43) and π_i^* ;
7: If $\frac{|\lambda_{s_t}^{i+1} - \lambda_{s_t}^i|}{\lambda_{s_t}^i} < \epsilon_2$. then $\pi = \pi_i^*$. Otherwise, increase i and go back to Step 2.

where β is a positive scalar step size satisfying the conditions $\sum_{i=1}^{\infty} \beta^i = \infty$ and $\sum_{i=1}^{\infty} (\beta^i)^2 < \infty$. The update rule is such that if $\sum_{n=1}^{N} \alpha_{n,t}^2$ is larger (smaller) than \mathcal{P}_{tot} then λ_{s_t} should increase (decrease). Unless the convergence criterion $\frac{|\lambda_{s_t}^{i+1} - \lambda_{s_t}^i|}{\lambda_{s_t}^i} < \epsilon_2$ is met, for a given ϵ_2 , we increase i and solve the inner maximization subproblem again.

Note that the above sub-gradient method is guaranteed to converge to the optimum λ_{s_t} , as long as β satisfies the conditions stated above, due to the convexity of the dual problem (42) over λ_{s_t} .

Remark on the computational complexity of Algorithm 1: We switch between solving two sub-problems until the convergence criterion for updating the Lagrangian multiplier is met. Given λ_{s_t} we solve the inner maximization sub-problem, i.e., we solve (40) for each $s_t \in \bar{\mathcal{S}}$ (refer to Step 3 of Algorithm 1), where $|\bar{\mathcal{S}}| = |\mathcal{S}|^N$. Our numerical results show that the computational complexity of calculating π_i^* (Step 5

of Algorithm 1) is $\mathcal{O}(|\mathcal{S}|^N K^{1.2N})$. On the other hand, the complexity order of the gradient-descent algorithm to find the local minimum of function $U(\lambda_{s_t})$ and converge to an ϵ_2 -accurate solution is $\bar{\epsilon} = 1/\epsilon_2$ [61, p. 232]. Hence, the overall computational complexity of finding the optimal policy using Algorithm 1 is $\mathcal{O}(\bar{\epsilon}|\mathcal{S}|^N K^{1.2N})$. Note that the complexity order scales *exponentially* in N.

Remark on implementing the optimal policy: The optimal policy, a.k.a. centralized solution in the dynamic control literature, requires the knowledge of the global state s_t to determine the network action $\alpha_t = \delta(s_t)$. This implies that sensor n in the network cannot find its local action $\alpha_{n,t}$ at time slot t, unless it knows the global state s_t . Hence, implementing this solution requires all N sensors to report their local states $s_{n,t}, \forall n$ to the FC. The FC concatenates all the received local states and forms the global state s_t . Then based on s_t , the FC determines and broadcasts the network action α_t . This process, however, consumes significant signaling overhead.

To reduce the signaling overhead, we consider finding a suboptimal policy, a.k.a. decentralized solution in the literature, where sensor n in the network finds its local action $\alpha_{n,t}$ at time slot t, only based on its own local state $s_{n,t}$.

B. Finding the Sub-Optimal Policy

Let δ'_n denote a deterministic decision rule that describes how a local action $\alpha_{n,t}$ of sensor n is selected according to the local state $s_{n,t}$ in time slot t, i.e., $\alpha_{n,t} = \delta'_n(s_{n,t})$, and $\omega_n = (\delta'_n, \delta'_n, ..., \delta'_n)$ be the corresponding stationary deterministic policy for t = 1, ..., T [57, pp.21]. We say that a policy ω_n is feasible if it satisfies the two constraints: (i) $\alpha_{n,t} \in \mathcal{U}_{n,t}$, $\forall t, n$, (ii) $\sum_{n=1}^{N} \alpha_{n,t}^2 \leq \mathcal{P}_{tot}$, $\forall t$. Let Ω be the set of feasible policies ω_n .

Our objective is to find a stationary deterministic policy $\omega_n \in \Omega$ that maximizes $V_{\omega_n}(s_1)$ in (44). We refer to this solution as the sub-optimal policy.

$$V_{\omega_n}(\mathbf{s}_1) = \mathbb{E}\left\{\sum_{t=1}^{\infty} \eta^t \sum_{n=1}^{N} r(\alpha_{n,t}) | \mathbf{s}_1, \pi\right\}, \forall n$$
s.t. $\alpha_{n,t} \in \mathcal{U}_{n,t}, \ \forall t, n, \ \sum_{n=1}^{N} \alpha_{n,t}^2 \le \mathcal{P}_{tot}, \ \forall t$ (44)

We note that maximizing $V_{\omega_n}(s_1)$ in (44) with respect to ω_n is simpler than maximizing $V_{\pi}(s_1)$ in (35) with respect to π , i.e., finding the sub-optimal policy is easier than finding the optimal policy. This is due to the fact that, when the local action $\alpha_{n,t}$ is selected according to the local state $s_{n,t}$ only in time slot t, the global state transition probability $\Pr\left(s_{t+1}|s_t,\alpha_t\right)$ in (7) can be completely decomposed across

$$\mathcal{X}(s_{n,t},\lambda) = \max_{\omega_n \in \Omega} \left\{ \underbrace{\mathcal{X}(s_{n,t},\alpha_{n,t},\lambda)}_{= \text{ term } 1} + \eta \Big(\Pr(\alpha_{n,t} = 0) \sum_{s_{n,t+1}} \Pr(s_{n,t+1}|s_{n,t},0) \mathcal{X}(s_{n,t+1},\lambda) + \Pr(\alpha_{n,t} \neq 0) \sum_{s_{n,t+1}} \Pr(s_{n,t+1}|s_{n,t},\alpha_{n,t}) \mathcal{X}(s_{n,t+1},\lambda) \Big) \right\},$$
(47)

sensors. In other words, we have

$$\Pr\left(s_{t+1}|s_{t},\alpha_{t}\right) = \prod_{n=1}^{N} \Pr\left(s_{n,t+1}|s_{n,t},\alpha_{n,t}\right) \qquad \qquad \min_{\lambda \geq 0} \widehat{U}(\lambda) \tag{49}$$

$$= \prod_{n=1}^{N} \Pr\left(b_{n,t+1}|b_{n,t},\bar{g}_{n,t},e_{n,t},\alpha_{n,t}\right) \Pr\left(\bar{g}_{n,t}|\bar{g}_{n,t-1}\right) \Pr\left(\bar{g}_{n,t}|\bar{g}_{n,t-1}\right) \text{ To solve the dual problem in (49), we iteratively solve the following two sub-problems until a pre-specified convergence criterion is reached. The outer minimization sub-problem until a pre-specified convergence criterion is reached. The outer minimization sub-problem until a pre-specified convergence criterion is reached. The outer minimization sub-problem until a pre-specified convergence criterion is reached.$$

where

$$\Pr\left(b_{n,t+1}|b_{n,t},\bar{g}_{n,t},e_{n,t},\alpha_{n,t}\right) = \begin{cases} 1 & \text{if (9) is satisfied} \\ 0 & \text{otherwise,} \end{cases}$$

The decomposition of the global state transition probability into the product of the local state transition probabilities directly impacts how the outer expectation $\mathbb{E}\{.\}$ in (44) is computed and allows the objective function in (44) to be decoupled across sensors. If there were no total transmit power constraint in (44), the MDP problem in (44) would have become completely decoupled across sensors. The challenge imposed by the total transmit power constraint can be addressed via adopting a uniform Lagrangian multiplier. Similar to [59] we let a uniform Lagrangian multiplier $\lambda_{s_t} = \lambda, \forall s_t$ be associated with the constraint $\left(\sum_{n=1}^{N} \alpha_{n,t}^2 - \mathcal{P}_{tot}\right)$. This uniform Lagrangian multiplier allows us to decouple the MDP problem in (44) across sensors and reduces solving (44) into solving N smaller MDP problems. While the computational complexity of finding the optimal policy scales exponentially in N, we will show that the computational complexity of finding the sub-optimal policy scales *linearly* in N.

We define the Lagrangian value function $\mathcal{X}(s_{n,t},\lambda)$ using the dynamic programming

$$\mathcal{X}(s_{n,t},\lambda) = \max_{\omega_n \in \Omega} \left\{ \underbrace{X(s_{n,t},\alpha_{n,t},\lambda)}_{\text{= term 1}} + \underbrace{\eta \sum_{s_{n,t+1}} \Pr\left(s_{n,t+1} | s_{n,t},\alpha_{n,t}\right) \mathcal{X}(s_{n,t+1},\lambda)}_{\text{= term 2}} \right\}, \quad (45)$$

where the modified reward function $X(s_{n,t}, \alpha_{n,t}, \lambda)$ is defined as

$$X(s_{n,t}, \alpha_{n,t}, \lambda) = r(\alpha_{n,t}) - \lambda \left(\alpha_{n,t}^2 - \frac{\mathcal{P}_{tot}}{N}\right)$$
(46)

With fixed λ , the constrained MDP problem in (44) can be viewed as N decoupled unconstrained MDP problems in (47) with the modified network reward function $X(s_{n,t}, \alpha_{n,t}, \lambda)$ at time slot t given in (46). Let $\widehat{U}(\lambda)$ denote the Lagrangian dual function, where

$$\widehat{U}(\lambda) = \max_{\omega_n \in \Omega} \mathcal{X}(s_{n,t}, \lambda) \tag{48}$$

Then the Lagrangian dual problem can be written as

$$\min_{\lambda \ge 0} \widehat{U}(\lambda) \tag{49}$$

updates λ^i . The inner maximization sub-problem finds the optimal $\omega_{n,i}$ given λ^i . The pseudo code of the algorithm is given in Algorithm 2.

- 1) the inner maximization problem: Given λ^i we adopt the value iteration algorithm [60] to find the sub-optimal policy $\omega_{n,i}$. The convergence criterion is $|\mathcal{X}^j(s_{n,t},\lambda)|$ $|\mathcal{X}^{j-1}(s_{n,t},\lambda)| < \epsilon_1(1-\eta)/2\eta$, for a given ϵ_1 , where $\mathcal{X}^{j}(s_{n,t},\lambda)$ indicates the long-term expected reward in the j-th iteration from (47).
- 2) the outer minimization problem: The outer minimization over the Lagrangian multiplier λ is a linear programming problem. We use the sub-gradient method to update λ^i as the following

$$\lambda^{i+1} = \left[\lambda^i + \beta^i \left(\sum_{n=1}^N \alpha_{n,t}^2 - \mathcal{P}_{tot}\right)\right]^+, \tag{50}$$

where β is a positive scalar step size satisfying the conditions $\sum_{i=1}^{\infty} \beta^i = \infty$ and $\sum_{i=1}^{\infty} (\beta^i)^2 < \infty$. The update rule is such that if $\sum_{n=1}^{N} \alpha_{n,t}^2$ is larger (smaller) than \mathcal{P}_{tot} then λ should increase (decrease). Unless the convergence criterion $\frac{|\lambda^{i+1}-\lambda^i|}{\lambda^i} < \epsilon_2$ is met, for a given ϵ_2 , we increase i and solve the inner maximization subproblem again.

Note that the above sub-gradient method is guaranteed to converge to the optimum λ , as long as β satisfies the conditions stated above.

Remark on the computational complexity of Algorithm 2: We switch between solving two sub-problems until the convergence criterion for updating the Lagrangian multiplier is met. Given λ we solve the inner maximization sub-problem, i.e., we solve (47) for each $s_{n,t} \in \mathcal{S}$ (refer to Step 3 of Algorithm 2), where the dimension of S, denoted as |S|. Our numerical results show that the computational complexity of calculating $\omega_{n,i}^*$ (Step 5 of Algorithm 2) is $\mathcal{O}(|\mathcal{S}|K^{1.5})$. On the other hand, the complexity order of the gradient-descent algorithm to find the local minimum of function $U(\lambda)$ and converge to an ϵ_2 -accurate solution is $\bar{\epsilon} = 1/\epsilon_2$ [61, p. 232]. Hence, the overall computational complexity of finding the sub-optimal policy using Algorithm 2 is $\mathcal{O}(\bar{\epsilon}N|\mathcal{S}|K^{1.5})$. Note that the complexity order scales *linearly* in N.

Remark on implementing the sub-optimal policy: The sub-optimal policy, a.k.a. decentralized solution in the dynamic control literature, requires the knowledge of the local state $s_{n,t}$ only to determine the local action $\alpha_{n,t} = \delta'_n(s_{n,t}), \forall n$. This

Algorithm 2: sub-optimal power control algorithm Inputs: $\mathcal{S}, \Phi_{\mathcal{E}}, \Psi_{\bar{\mathcal{G}}}^{(n)}, K, \gamma_{g_n}, \sigma_{w_n}^2, \mathcal{P}_{tot}, P_{\mathbf{f}_n}, P_{\mathbf{d}_n}, \eta, \epsilon_1, \epsilon_2$ Output: sub-optimal policy ω_n

1: Specify
$$\epsilon_1 > 0$$
, $\epsilon_2 > 0$ set $\mathcal{X}(s_{n,0}, \lambda) = 0$, $s_{n,t} \in \mathcal{S}$ set $i = 1$;

2: **for** fixed λ^i **do**

3: Set
$$j=1$$
, for each sensor do for each $\alpha_{n,t} \in \mathcal{U}_{s_{n,t}}$ do calculate
$$\mathcal{F}(s_{n,t},\alpha_{n,t},\lambda^i) = X(s_{n,t},\alpha_{n,t}\lambda) + \\ \eta\Big(\sum_{s_{t+1}} \Pr(s_{n,t+1}|s_{n,t},\alpha_{n,t})\mathcal{X}^{j-1}(s_{n,t+1},\lambda^i)\Big)$$
 end calculate
$$\mathcal{X}^j(s_{n,t},\lambda^i) = \max_{\omega_{n,i} \in \Omega} \{\mathcal{F}(s_{n,t},\alpha_{n,t},\lambda^i)\}$$
 end 4: If

$$\max_{s_{n,t} \in \mathcal{S}} |\mathcal{X}^j(s_{n,t}, \lambda^i) - \mathcal{X}^{j-1}(s_{n,t}, \lambda^i)| < \epsilon_1(1 - \eta)/2\eta$$

go to step 5. Otherwise, increase j and go back to Step 3.

5: We obtain policy

$$\omega_{n,i}^* = \arg\max_{\omega_{n,i} \in \Omega} \left\{ \mathcal{X}^j(s_{n,t}) \right\}.$$

end

6: Update λ^i by using (50) and $\omega_{n,i}^*$; 7: If $\frac{|\lambda^{i+1} - \lambda^i|}{\lambda^i} < \epsilon_2$ then $\omega_n = \omega_{n,i}^*$. Otherwise, increase i and go back to Step 2.

implies that sensor n in the network can find its local action $a_{n,t}$ at time slot t with the knowledge of its local state $s_{n,t}$. Hence, implementing this solution, different from the optimal solution, does not require sensors to report to the FC and does not impose signaling overhead to the sensors.

IV. EFFECT OF RANDOM DEPLOYMENT OF SENSORS

Our signal model in (1) is a widely adopted model in the literature of signal (target) detection [12], [15], [62], in which the signal source is typically modeled as an isotropic radiator and the emitted power of the signal source at a reference distance d_0 is known [63]. Suppose P_0 is the emitted power of the signal source at the reference distance d_0 , and d_n is the Euclidean distance between the source and sensor n. For a general intensity decay model, the signal intensity at sensor n, denoted as $z_{n,t}$, is [63]

$$z_{n,t} = \frac{P_0}{(d_n/d_0)^{\gamma}},\tag{51}$$

where γ is the path-loss exponent, e.g., for free-space wave propagation $\gamma = 2$. With this model, the problem of noisy signal detection is equivalent to the following binary hypothesis testing problem

$$H_t = 1: x_{n,t} = z_{n,t} + v_{n,t}, H_t = 0: x_{n,t} = v_{n,t}, (52)$$

in which $z_{n,t}$ and variance of $v_{n,t}$, denoted as $\sigma^2_{v_n}$, are assumed to be known [12], [15], [62]. Note that the binary hypothesis testing problem in (52) can be recast as the problem in (1), by scaling the sensor observation $x_{n,t}$ with $(d_n/d_0)^{\gamma}$. This signal model applies to an arbitrary, but fixed (given) deployment of sensors. For applications where the sensors are deployed randomly in a field, the sensors' locations are not known a prior. This implies that A in (1) is unknown, and consequently, $P_{\mathbf{f}_n}$ in (4) cannot be determined before deployment. To expand our optimization method beyond fixed deployment of sensors, we assume that sensors are randomly deployed in a circle field, the signal source is located at the center of this field, and it is at least r_0 meters away from any sensor within the field. Let $r_{n,t}$ be the distance of sensor n from the center. We assume $r_{n,t}$ is uniformly distributed in the interval (r_0, r_1) , i.e.,

$$f(r_{n,t}) = \begin{cases} \frac{1}{r_1 - r_0}, & r_0 < r_{n,t} \le r_1, \\ 0, & \text{o.w.} \end{cases}$$
 (53)

Suppose the emitted power of the signal source at radius r_0 is P_0 . Then the signal intensity at sensor n is $z_{n,t} = \frac{P_0}{(r_{n,t}/r_0)^2}$. Given the pdf of $r_{n,t}$ in (53), we obtain the pdf of $z_{n,t}$ as

$$f(z_{n,t}) = \begin{cases} \frac{\sqrt{P_0}}{2z_{n,t}\sqrt{z_{n,t}}(r_1 - r_0)}, & \frac{P_0}{r_1^2} < z_{n,t} \le \frac{P_0}{r_0^2}, \\ 0, & \text{o.w.} \end{cases}$$
(54)

Based on the pdf of $z_{n,t}$ in (54) we can recompute $P_{\mathbf{f}_n}$ in (4)

$$P_{f_n} = \int_{\frac{P_0}{r_1^2}}^{\frac{P_0}{r_0^2}} \left[Q\left(\frac{\theta_n + \frac{z_{n,t}^2}{2\sigma_{v_n}^2}}{\sqrt{z_{n,t}^2/\sigma_{v_n}^2}}\right) \right] f(z_{n,t}) dz_{n,t},$$

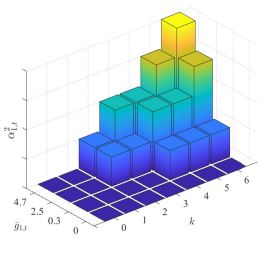
$$P_{d_n} = \int_{\frac{P_0}{r_1^2}}^{\frac{P_0}{r_0^2}} \left[Q\left(\frac{\theta_n - \frac{z_{n,t}^2}{2\sigma_{v_n}^2}}{\sqrt{z_{n,t}^2/\sigma_{v_n}^2}}\right) \right] f(z_{n,t}) dz_{n,t},$$
 (55)

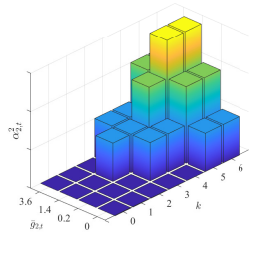
$$P_{\rm f_n} = \int_{\frac{P_0}{r^2}}^{\frac{P_0}{r_0^2}} Q\left(Q^{-1}(\overline{P}_{\rm d}) + \sqrt{z_{n,t}^2/\sigma_{v_n}^2}\right) f(z_{n,t}) dz_{n,t}.$$
 (56)

With random deployment of sensors, problem (P1) is still valid, with the difference that, for $J_{n,t}$ in (21), P_{f_n} expression should be replaced with the ones in (55)-(56).

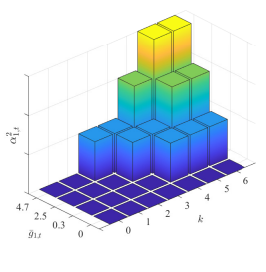
V. SIMULATION RESULTS

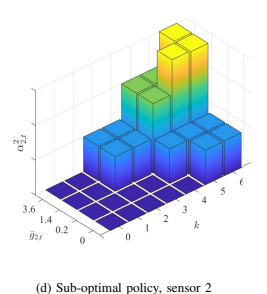
We corroborate our analysis with MATLAB simulations and investigate: (i) the effect of policy (optimal versus sub-optimal) on transmit powers of sensors, (ii) the achievable J-divergence when we adopt the optimal, and sub-optimal, and random policies to set transmit powers of sensors, (iii) error probability P_e when we adopt the optimal and sub-optimal policies to set transmit powers of sensors, and the trade-off between P_e and consumed transmit power, (iv) the behavior of P_e as different system parameters vary, (v) the effect of random deployment of sensors on P_e .





 $0.04, L = 4, \vec{\mathcal{G}_1} = \{0, 0.3, 2.5, 4.7\}, \vec{\mathcal{G}_2} = \{0, 0.2, 1.4, 3.6\}, \ (\rho_1, \rho_2) = (0.4, 0.5), (e_{1,t}, e_{2,t}) = (2b_u, 2b_u).$





(a) Optimal policy, sensor 1

(b) Optimal policy, sensor 2 (c) Sub-optimal policy, sensor l

Fig. 5: Transmit powers $(\alpha_{1,t}^2,\alpha_{2,t}^2)$ in optimal and sub-optimal policies for N=2, $SNR_s=3dB$, $\mathcal{P}_{tot}=5mW$, K=6, $b_u=0.5mJ$, $(\gamma_{g_1},\gamma_{g_2})=(1,1.5)$, $f_DT_s=0.5mJ$

In all our simulations, we let $\sigma_{w_n}^2 = \sigma_w^2 = 1, \forall n$ and $P_{d_n} = P_d, \forall n$. Also, $\gamma_{g_n}^2 = \gamma_g^2, \forall n$ except for Fig. 5. We let $P_d = 0.9$ except for Fig. 10, the discount factor $\eta = 0.9$ except for Fig. 14, and $f_D T_s = 0.05$ except for Fig. 10. We assume the Gaussian observation noise variance $\sigma_{v_n}^2 = \sigma_v^2, \forall n$ and we define the SNR corresponding to observation channel as $\mathrm{SNR}_s = 20 \log(\mathcal{A}/\sigma_v)$. We adopt a solar-power energy harvesting model similar to [54], in which the harvesting condition is classified to M=4 states as "Poor", "Fair", "Good", and "Excellent". We assume $\mathcal{E} = \{0, 2b_u, 4b_u, 6b_u\}$ and the transition probability matrix $\Phi_{\mathcal{E}}$ is characterized in

$$\Phi_{\mathcal{E}} = \begin{pmatrix} \rho & 1 - \rho & 0 & 0\\ \frac{1-\rho}{2} & \rho & \frac{1-\rho}{2} & 0\\ 0 & \frac{1-\rho}{2} & \rho & \frac{1-\rho}{2}\\ 0 & 0 & 1 - \rho & \rho \end{pmatrix}.$$

terms of an energy harvesting parameter ρ as the following

We let $\rho=0.5$ except for Figs. 5 and 15. Our battery-related parameters are (K,b_u) . Our system setup is based on a given set of L channel gain quantization thresholds $\bar{\mathcal{G}}=\{\mu_1,\mu_2,...,\mu_L\}$. To explore the effect of quantization thresholds we consider two different objective functions to obtain the quantization thresholds $\{\mu_l\}_{l=1}^L$.

• Finding $\{\mu_l\}_{l=1}^L$ via Minimizing Mean Absolute Error (MMAE): We consider mean of absolute quantization error (MAE), denoted as $\mathbb{E}\{|g_{n,t}-\bar{g}_{n,t}|\}$, as the objective function

$$\mathbb{E}\{|g_{n,t} - \bar{g}_{n,t}|\} = \sum_{l=0}^{L-1} \int_{\mu_l}^{\mu_{l+1}} (x - \mu_l) f_{g_{n,t}}(x) dx.$$
 (57)

To find $\{\mu_l\}_{l=1}^L$ that minimize MAE, we take the derivative of MAE with respect to μ_l and set the derivative equal to zero.

• Finding $\{\mu_l\}_{l=1}^L$ via Maximizing output Entropy (MOE): We consider the mutual information between $g_{n,t}$ and $\bar{g}_{n,t}$, denoted as $I(g_{n,t};\bar{g}_{n,t})$, as the objective function, where $I(g_n;\bar{g}_{n,t})=H(\bar{g}_{n,t})-H(\bar{g}_{n,t}|g_{n,t})$, and H(x) denotes the entropy of discrete random variable x. To find $\{\mu_l\}_{l=1}^L$ that maximize $I(g_{n,t};\bar{g}_{n,t})$, we note that $H(\bar{g}_{n,t}|g_{n,t})$ is zero, since given $g_{n,t}$, $\bar{g}_{n,t}$ is known. Furthermore, $H(\bar{g}_{n,t})$ is maximized when $\bar{g}_{n,t}$ follows a uniform distribution, i.e., we set $\phi_{n,l}=\Pr(\bar{g}_{n,t}=\mu_l)=\Pr(\mu_l\leq g_{n,t}<\mu_{l+1})=\frac{1}{L+1}$, and the threshold μ_l can be obtained as $\mu_l=\left(-\gamma_{g_n}\ln\left(1-\frac{l-1}{L+1}\right)\right)^{\frac{1}{2}}$. Overall, our channel-related parameters are $(\gamma_{g_n},f_DT_s,L,\bar{\mathcal{G}})$, where $\bar{\mathcal{G}}$ depends on (γ_{g_n},L) and the choice of objective function to obtain the quantization

thresholds. The state probabilities and the entries of the transition probability matrix $\Psi_{\bar{\mathcal{G}}}^{(n)}$ can be obtained via (5)-(6) given $(\gamma_{g_n}, f_D T_s, L, \bar{\mathcal{G}})$.

- Effect of policy on transmit powers of sensors: To show how transmit power $\alpha_{n,t}^2$ of sensor n changes based on the adopted policy, we consider N=2 sensors. Recall for the sub-optimal policy $\alpha_{n,t}$ depends on the local state $s_{n,t} = (b_{n,t}, \bar{g}_{n,t-1}, e_{n,t-1})$, whereas for the optimal policy the local action $\alpha_{n,t}$ depends on the global state $s_t = (s_{1,t}, s_{2,t})$. We use Algorithm 1 and Algorithm 2, to find and set transmit power $\alpha_{n,t}^2$ corresponding to the optimal and the sub-optimal policies, respectively. Fig. 5 illustrates $(\alpha_{1,t}^2, \alpha_{2,t}^2)$ when optimal and sub-optimal policies are adopted, given a set of energy harvesting, battery-related, and channel-related parameters, and assuming the quantization thresholds are obtained via MMAE. To enable the illustration, we assume the state of energy harvesting for both sensors is "Fair", i.e., $(e_{1,t-1}, e_{2,t-1}) = (2b_u, 2b_u)$, and the states of battery $(b_{1,t}, b_{2,t})$ and the states of quantized channel gains $(\bar{g}_{1,t-1},\bar{g}_{2,t-1})$ are variable. For example, this figure shows that when the local states are $s_{1,t} = (7,3,2), s_{2,t} =$ (7,3,2), then transmit powers of sensors corresponding to the optimal policy is $(\alpha_{1,t}, \alpha_{2,t}) = (1.5 \text{mW}, 2 \text{mW})$, whereas transmit powers of sensors corresponding to the sub-optimal policy is $(\alpha_{1,t}, \alpha_{2,t}) = (1\text{mW}, 3\text{mW})$. The Achievable J_{tot} corresponding to optimal and sub-optimal policies are 11.58 and 10.43, respectively. These figures also show that, $\alpha_{n,t}^2(b_{n,t},\bar{g}_{n,t-1},e_{n,t-1})$ is monotonically increasing in $b_{n,t}$, given $\bar{g}_{n,t-1}$ and $e_{n,t-1}$.
- Achievable J-divergence corresponding to optimal, sub-optimal, and random policies: Fig. 6 and Fig. 7 show average J-divergence versus b_u and SNR $_s$ respectively. To plot the curves we set transmit power $\alpha_{n,t}^2$ corresponding to the optimal, the sub-optimal, and random policies, and then we average $J_{tot,t} = \sum_{n=1}^N J_{n,t}$ over 10^4 independent Monte Carlo runs. For random policy, we randomly choose $\alpha_{n,t}^2$ such that the two constraints in (34) are satisfied, i.e., (i) $\alpha_{n,t}^2 T_s/b_u \leq b_{n,t}, \ \forall t,n,$ (ii) $\sum_{n=1}^N \alpha_{n,t}^2 \leq \mathcal{P}_{tot}, \ \forall t$. Fig. 6 illustrates that, given a K value, the average J-divergence increases in b_u , however, it remains almost the same after b_u reaches and exceeds a certain value. This is due to the fact that, for larger b_u values transmit power is not limited by energy harvesting and stored energy. Instead, it is limited by the communication channel noise variance σ_w^2 . Fig. 7 shows

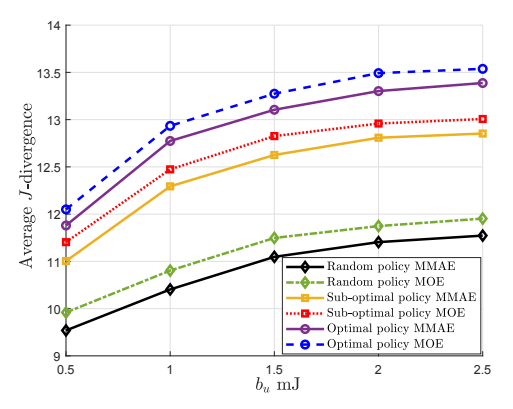


Fig. 6: The average J-divergence versus b_u for $K=5, N=3, \mathcal{P}_{tot}=5 \text{mW}, \gamma_g=2, L=3, \text{SNR}_s=3 \text{dB}$.

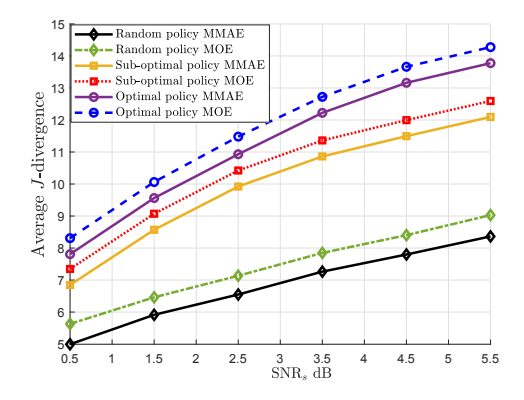


Fig. 7: The average J-divergence versus ${\rm SNR}_s$ dB for $K=5,~N=3, \mathcal{P}_{tot}=5{\rm mW}, b_u=1{\rm mJ}, \gamma_g=2, L=3.$

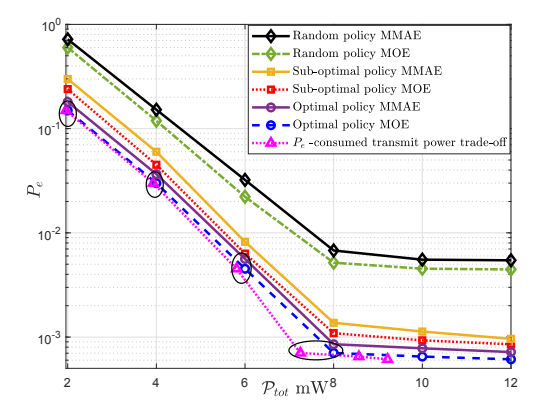


Fig. 8: P_e versus \mathcal{P}_{tot} for K=5, N=3, $b_u=1$ mJ, $\gamma_g=2$, L=3, $\mathrm{SNR}_s=3$ dB.

that the average J-divergence increases in SNR $_s$. This is due to the fact that as SNR $_s$ increases, $P_{f_n} = P_f$, $\forall n$ in (4) decreases (given a P_d value). Decreasing P_f leads into increasing the average J-divergence, where P_f and $J_{n,t}$ are related through (21) and (22). In both figures, average J-divergence achieved by the sub-optimal policy is smaller than average J-divergence achieved by the optimal policy, and larger than average J-divergence achieved by the random policy.

• P_e corresponding to optimal and sub-optimal policies, and P_e -consumed transmit power trade-off: Fig. 8 shows P_e versus \mathcal{P}_{tot} . To plot the curves we set transmit power $\alpha_{n\ t}^2$

corresponding to the optimal and the sub-optimal policies, and then we consider 10^4 independent Monte Carlo runs to find P_e , i.e., we generate 10^4 realizations of random noises and fading channels and count the errors, P_e is the number of errors occurred divided by 10^4 . Fig. 8 reveals two important points: (i) "optimal policy MOE" and "optimal policy MMAE" achieve the lowest P_e , followed by "sub-optimal policy MOE" and "sub-optimal policy MMAE", followed by "random policy MOE" and "random policy MMAE", (ii) "sub-optimal policy" performs very close to "optimal policy". Note that for all curves, P_e decreases as \mathcal{P}_{tot} increases, however, it reaches an error floor after \mathcal{P}_{tot} exceeds a certain value. This is due to the fact that for larger \mathcal{P}_{tot} values, P_e is not limited by \mathcal{P}_{tot} . Instead, it is limited by σ_w^2 .

Fig. 8 also allows us to examine the existing trade-off between the consumed transmit power and P_e . Consider the curve labeled " P_e -consumed transmit power trade-off" in Fig. 8, which shows how much transmit power is required to provide a certain P_e value. This curve is obtained from examining the points on "optimal policy MOE" and checking whether the constraint $\sum_{n=1}^{N} \alpha_{n,t}^2 \leq \mathcal{P}_{tot}$, $\forall t$. is active or inactive. At a given point, when this constraint is active (inactive), the consumed transmit power is equal to (less than) \mathcal{P}_{tot} . Note that as \mathcal{P}_{tot} increases and P_e reaches an error floor, the consumed transmit power is less than \mathcal{P}_{tot} .

Since finding the sub-optimal policy has a much lower computational complexity than that of the optimal policy, and its performance is very close to the optimal policy, from this point forward, we focus on the sub-optimal policy.

• Dependency of P_e on different system parameters: Fig. 9-12 plot P_e corresponding to sub-optimal policy in terms of different system parameters. Fig. 9 depicts P_e versus K as γ_g and b_u change. Given the pair (γ_g,b_u) , P_e decreases as K increases, until it reaches an error floor. The error floor becomes smaller as (i) γ_g increases, given b_u , (ii) b_u increases, given γ_g . The presence of error floor is due to the fact that, for larger K values P_e is no longer restricted by K, and instead it is restricted by σ_w^2 , leading to an error floor.

Fig. 10 depicts P_e versus N as f_DT_s and P_d vary. We observe that, given the pair (f_DT_s, P_d) , P_e reduces when N increases, however, it reaches an error floor after cretin value of N. This is due to the fact that for larger N values, P_e becomes limited by \mathcal{P}_{tot} and σ_w^2 . Furthermore, we notice that P_e decreases when (i) given the pair (N, P_d) , f_DT_s increases; (ii) given the pair (N, f_DT_s) , P_d increases.

Fig. 11 shows P_e versus SNR_s as L,N change. Examination of this figure shows that P_e reduces when (i) given the pair (L,N), SNR_s increases. This is because as SNR_s increases, $P_{f_n} = P_f, \forall n$ in (4) decreases, (ii) given the pair (SNR_s, L), N increases, (iii) given the pair (SNR_s, N), L increases. This is because as L increases the feedback information from the FC to the sensors on channel gain increases.

Fig. 12 shows P_e versus η as γ_g varies. Given γ_g , P_e decreases in η . This is due to the fact that, as η increases, the sub-optimal $\alpha_{n,t}^2$ values increases, leading to a decrease in P_e .

We note that there is a performance-computational complexity trade-off as η increases. Recall the mean of the network

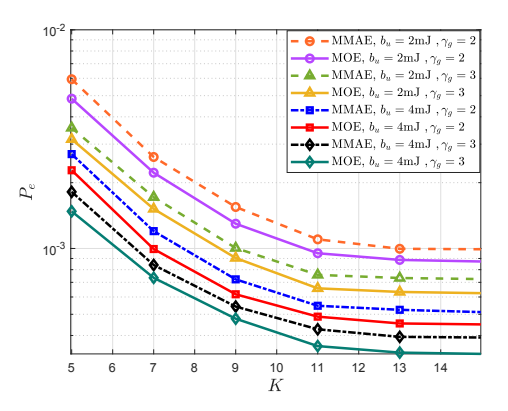


Fig. 9: P_e vs. K for N = 10, $\mathcal{P}_{tot} = 15$ mW, L = 4, $\text{SNR}_s = 5$ dB.

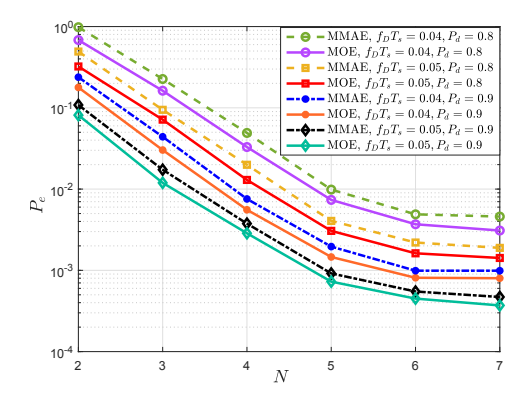


Fig. 10: P_e vs. N for $K=10, \mathcal{P}_{tot}=15 \mathrm{mW},~b_u=2 \mathrm{mJ}~\gamma_g=1.5, L=4, \mathrm{SNR}_s=3 \mathrm{dB}.$

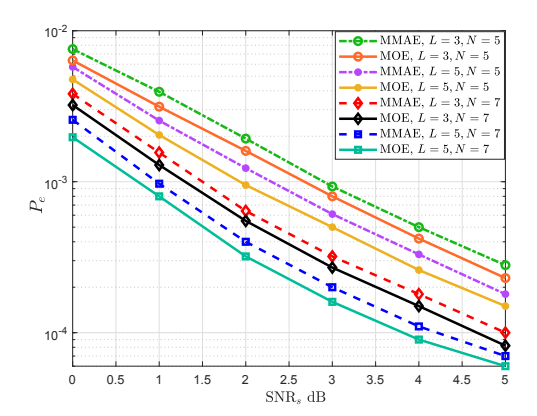


Fig. 11: P_e vs. ${\rm SNR}_s$ for $K=10, \mathcal{P}_{tot}=15$ mW, $b_u=2$ mJ, $\gamma_g=2$.

lifetime T is $\mathbb{E}\{T\} = 1/(1-\eta)$. As η increases, the number of iterations required for the value iteration algorithm (i.e., step 3 of Algorithm 2) to converge increases.

• Cannot a node consume all its stored energy?: Given the constraint $\sum_{n=1}^{N} \alpha_{n,t}^2 \leq \mathcal{P}_{tot}$, $\forall t$ the answer is no. When one relaxes this constraint, the proposed optimal and sub-optimal policies become the same and the outputs of Algorithms 1 and 2 become identical. Let new optimal policy denote the algorithm output when the constraint is relaxed, and greedy-based policy be the policy in which sensor n in time slot t uses all its available energy for transmission, i.e., $\alpha_{n,t} = \sqrt{b_{n,t}b_u/T_s}$. Fig. 13 plots P_e corresponding to new

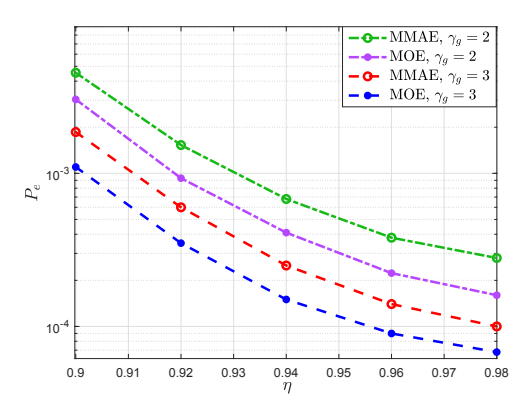


Fig. 12: P_e vs. η for $K=10, N=5, \mathcal{P}_{tot}=15$ mW, $b_u=1, L=4$, SNR $_s=3$ dB.

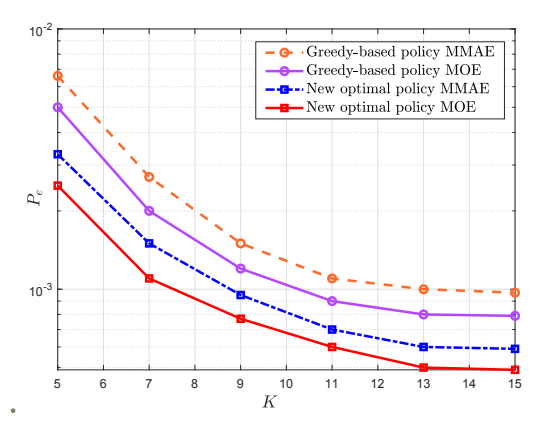


Fig. 13: P_e vs. K for $N=10, L=4, b_u=3mJ, \gamma_g=2$ SNR $_s=5$ dB.

optimal policy and greedy-based policy versus K. Clearly, new optimal policy outperforms greedy-based policy.

• Effect of random deployment of sensors on P_e : We consider a circle field where the signal source with power P_0 is located at its center. Sensors are randomly deployed in the field such that the distance of sensor n from the source, r_n , is uniformly distributed in the interval of $(r_0, r_1) = (1 \text{m}, 100 \text{m})$. We assume the quantization thresholds are obtained via MMAE. Fig. 14 illustrates P_e versus P_0 as γ_g and b_u change. We observe that P_e decreases when: (i) given the pair (γ_g, b_u) , P_0 increases, (ii) given the pair (P_0, b_u) , γ_g increases, (iii) given the pair (P_0, γ_g) , b_u increases. These observations are all expected.

Fig. 15 illustrates P_e versus N for fixed and random deployment, as ρ and K vary. For the given set of parameters, the performance of fixed and random deployments is close to each other. Also, given the pair (ρ,K) , P_e reduces when N increases, however, it reaches an error floor after N exceeds a certain value. This is due to the fact that for larger N values, P_e becomes limited by \mathcal{P}_{tot} and σ_w^2 . Furthermore, we notice that P_e decreases when (i) given the pair (N,K), ρ increases, (ii) given the pair (N,ρ) , K increases.

VI. CONCLUSIONS

Considering an EH-enabled WSN with N sensors and a feedback channel from the FC to the sensors, tasked with binary distributed detection, we developed adaptive channel-

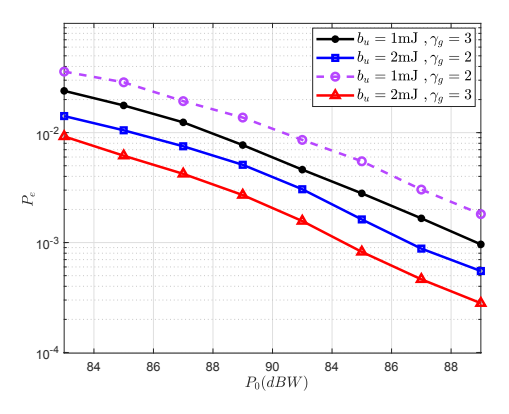


Fig. 14: P_e vs. P_0 for K = 10, N = 5, $\mathcal{P}_{tot} = 15$ mW, L = 4, $(r_0, r_1) = (1$ m, 100m).

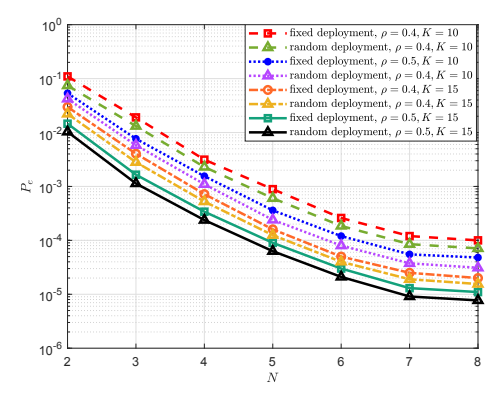


Fig. 15: P_e vs. N for $\mathcal{P}_{tot}=15\text{mW}, b_u=4\text{mJ}, \gamma_g=1.5, L=4$ (i) for fixed deployment $\text{SNR}_s=5\text{dB}, P_{\text{d}}=0.9$, (ii) for random deployment $(r_0,r_1)=(1\text{m},100\text{m}), P_0=84\text{dBW}$

dependent transmit power control policies such that the detection performance is optimized, subject to total transmit power constraint. Modeling the quantized fading channel, the energy arrival, and the dynamics of the battery as homogeneous FSMCs, and the network lifetime as a random variable with geometric distribution, we formulated our power control optimization problem as a discounted infinite-horizon constrained MDP problem, where sensors' transmit powers are functions of the battery state, quantized CSI, and the arrived energy. We developed the optimal policy, using dynamic programming and utilizing the Lagrangian approach to transform the constrained MDP problem into an equivalent unconstrained MDP problem. Determining the optimal policy, however, requires the knowledge of the global state at the FC, which imposes a significant signaling overhead to the sensors. To eliminate this overhead, we developed the sub-optimal policy, using a uniform Lagrangian multiplier to transform the constrained MDP problem into N unconstrained MDP problems. Different from the optimal policy, in the sub-optimal policy each sensor sets its transmit power based on its local state information. We showed that the computational complexity of finding the suboptimal policy scales linearly in N and this policy has a closeto-optimal performance. We studied the error probability P_e in terms of different system parameters, including K, N, \mathcal{P}_{tot} , SNR_s . Although P_e decreases as each of these parameters increases, there is an error floor that ultimately depends on the

communication channel noise variance and \mathcal{P}_{tot} . We expanded our work to random deployment of sensors and examined how it affects the error probability. The insights obtained in this work are useful for adaptive transmit power control of EH-enabled WSNs tasked with distributed detection.

REFERENCES

- D. Ciuonzo, P. S. Rossi, and P. K. Varshney, "Distributed detection in wireless sensor networks under multiplicative fading via generalized score tests," *IEEE Internet of Things Journal*, vol. 8, no. 11, pp. 9059– 9071, 2021.
- [2] H. R. Ahmadi and A. Vosoughi, "Distributed detection with adaptive topology and nonideal communication channels," *IEEE transactions on signal processing*, vol. 59, no. 6, pp. 2857–2874, 2011.
- [3] Y.-W. Kuo, C.-L. Li, J.-H. Jhang, and S. Lin, "Design of a wireless sensor network-based iot platform for wide area and heterogeneous applications," *IEEE Sensors Journal*, vol. 18, no. 12, pp. 5187–5197, 2018
- [4] M. A. Al-Jarrah, M. A. Yaseen, A. Al-Dweik, O. A. Dobre, and E. Alsusa, "Decision fusion for IoT-based wireless sensor networks," *IEEE Internet of Things Journal*, vol. 7, no. 2, pp. 1313–1326, 2019.
- [5] P. K. Varshney, "Distributed detection and data fusion," 1996.
- [6] J. N. Tsitsiklis, "Decentralized detection by a large number of sensors," Mathematics of Control, Signals and Systems, vol. 1, no. 2, pp. 167–182, 1088
- [7] R. Viswanathan and P. K. Varshney, "Distributed detection with multiple sensors part i. fundamentals," *Proceedings of the IEEE*, vol. 85, no. 1, pp. 54–63, 1997.
- [8] B. Chen, L. Tong, and P. K. Varshney, "Channel-aware distributed detection in wireless sensor networks," *IEEE Signal Processing Magazine*, vol. 23, no. 4, pp. 16–26, 2006.
- [9] R. Niu, B. Chen, and P. K. Varshney, "Fusion of decisions transmitted over rayleigh fading channels in wireless sensor networks," *IEEE Transactions on signal processing*, vol. 54, no. 3, pp. 1018–1027, 2006.
- [10] Z. Hajibabaei, A. Vosoughi, and N. Mastronarde, "Optimal power allocation for M-ary distributed detection in the presence of channel uncertainty," *Signal Processing*, vol. 169, p. 107400, 2020.
- [11] H. R. Ahmadi and A. Vosoughi, "Impact of channel estimation error on decentralized detection in bandwidth constrained wireless sensor networks," in MILCOM 2008-2008 IEEE Military Communications Conference. IEEE, 2008, pp. 1–7.
- [12] X. Zhang, H. V. Poor, and M. Chiang, "Optimal power allocation for distributed detection over mimo channels in wireless sensor networks," *IEEE Transactions on Signal Processing*, vol. 56, no. 9, pp. 4124–4140, Sep. 2008.
- [13] H.-s. Kim and N. A. Goodman, "Power control strategy for distributed multiple-hypothesis detection," *IEEE Transactions on Signal Processing*, vol. 58, no. 7, pp. 3751–3764, 2010.
- [14] H. R. Ahmadi, N. Maleki, and A. Vosoughi, "On power allocation for distributed detection with correlated observations and linear fusion," *IEEE Transactions on Vehicular Technology*, vol. 67, no. 9, pp. 8396– 8410, 2018.
- [15] N. Maleki and A. Vosoughi, "On bandwidth constrained distributed detection of a known signal in correlated gaussian noise," *IEEE Trans*actions on Vehicular Technology, 2020.
- [16] V. W. Cheng and T.-Y. Wang, "Performance analysis of distributed decision fusion using a censoring scheme in wireless sensor networks," *IEEE Transactions on Vehicular Technology*, vol. 59, no. 6, pp. 2845– 2851, 2010.
- [17] Z. Wang, V. Aggarwal, and X. Wang, "Iterative dynamic water-filling for fading multiple-access channels with energy harvesting," *IEEE Journal* on Selected Areas in Communications, vol. 33, no. 3, pp. 382–395, 2015.
- [18] M.-L. Ku, W. Li, Y. Chen, and K. R. Liu, "Advances in energy harvesting communications: Past, present, and future challenges," *IEEE Communications Surveys & Tutorials*, vol. 18, no. 2, pp. 1384–1412, 2015.
- [19] H. Yazdani and A. Vosoughi, "Steady-state rate-optimal power adaptation in energy harvesting opportunistic cognitive radios with spectrum sensing and channel estimation errors," *IEEE Transactions on Green Communications and Networking*, 2021.
- [20] M. Nourian, S. Dey, and A. Ahlén, "Distortion minimization in multisensor estimation with energy harvesting," *IEEE Journal on Selected Areas in Communications*, vol. 33, no. 3, pp. 524–539, 2015.

- [21] J. Geng and L. Lai, "Non-bayesian quickest change detection with stochastic sample right constraints," *IEEE Transactions on Signal Pro*cessing, vol. 61, no. 20, pp. 5090–5102, 2013.
- [22] S. S. Gupta, S. K. Pallapothu, and N. B. Mehta, "Ordered transmissions for energy-efficient detection in energy harvesting wireless sensor networks," *IEEE Transactions on Communications*, vol. 68, no. 4, pp. 2525–2537, 2020.
- [23] A. Tarighati, J. Gross, and J. Jaldén, "Decentralized hypothesis testing in energy harvesting wireless sensor networks," *IEEE Transactions on Signal Processing*, vol. 65, no. 18, pp. 4862–4873, Sep. 2017.
- [24] Q. Duan, X. Liu, and H. Wang, "Adaptive transmission control strategy for distributed detection in EH-WSNs," in 2022 7th International Conference on Intelligent Computing and Signal Processing (ICSP), 2022, pp. 571–575.
- [25] G. Ardeshiri, H. Yazdani, and A. Vosoughi, "Optimal local thresholds for distributed detection in energy harvesting wireless sensor networks," in 2018 IEEE Global Conference on Signal and Information Processing (GlobalSIP), Nov 2018, pp. 813–817.
- [26] G. Ardeshiri, H. Yazdani, and A. Vosoughi, "Power adaptation for distributed detection in energy harvesting wsns with finite-capacity battery," in 2019 IEEE Global Communications Conference (GLOBECOM). IEEE, 2019, pp. 1–6.
- [27] G. Ardeshiri and A. Vosoughi, "On adaptive transmission for distributed detection in energy harvesting wireless sensor networks with limited fusion center feedback," *IEEE Transactions on Green Communications* and Networking, vol. 6, no. 3, pp. 1764–1779, 2022.
- [28] O. Ozel, K. Tutuncuoglu, J. Yang, S. Ulukus, and A. Yener, "Transmission with energy harvesting nodes in fading wireless channels: Optimal policies," *IEEE Journal on Selected Areas in Communications*, vol. 29, no. 8, pp. 1732–1743, Sep. 2011.
- [29] T. Banerjee, P. Gurram, and G. T. Whipps, "A bayesian theory of change detection in statistically periodic random processes," *IEEE Transactions* on *Information Theory*, vol. 67, no. 4, pp. 2562–2580, 2021.
- [30] K. Premkumar and A. Kumar, "Optimal sleep-wake scheduling for quickest intrusion detection using wireless sensor networks," in *IEEE INFOCOM 2008-The 27th Conference on Computer Communications*. IEEE, 2008, pp. 1400–1408.
- [31] Z. Wang, V. Aggarwal, and X. Wang, "Iterative dynamic water-filling for fading multiple-access channels with energy harvesting," *IEEE Journal* on Selected Areas in Communications, vol. 33, no. 3, pp. 382–395, 2015.
- [32] D. Zhao, C. Huang, Y. Chen, F. Alsaadi, and S. Cui, "Resource allocation for multiple access channel with conferencing links and shared renewable energy sources," *IEEE Journal on Selected Areas in Communications*, vol. 33, no. 3, pp. 423–437, 2015.
- [33] J. Yang, O. Ozel, and S. Ulukus, "Broadcasting with an energy harvesting rechargeable transmitter," *IEEE Transactions on Wireless Communications*, vol. 11, no. 2, pp. 571–583, 2011.
- [34] O. Ozel, J. Yang, and S. Ulukus, "Optimal broadcast scheduling for an energy harvesting rechargeable transmitter with a finite capacity battery," *IEEE Transactions on Wireless Communications*, vol. 11, no. 6, pp. 2193–2203, 2012.
- [35] J. Rubio and A. Pascual-Iserte, "Energy-aware broadcast multiuser-mimo precoder design with imperfect channel and battery knowledge," IEEE transactions on wireless communications, vol. 13, no. 6, pp. 3137–3152, 2014.
- [36] A. Ikhlef, "Optimal mimo multicast transceiver design for simultaneous information and power transfer," *IEEE Communications Letters*, vol. 18, no. 12, pp. 2153–2156, 2014.
- [37] K. Tutuncuoglu and A. Yener, "Sum-rate optimal power policies for energy harvesting transmitters in an interference channel," *Journal of Communications and Networks*, vol. 14, no. 2, pp. 151–161, 2012.
- [38] P. S. Khairnar and N. B. Mehta, "Discrete-rate adaptation and selection in energy harvesting wireless systems," *IEEE Transactions on Wireless Communications*, vol. 14, no. 1, pp. 219–229, 2014.
- [39] S. Rao and N. B. Mehta, "Hybrid energy harvesting wireless systems: Performance evaluation and benchmarking," *IEEE Transactions on Wireless Communications*, vol. 13, no. 9, pp. 4782–4793, 2014.
- [40] C. Huang, R. Zhang, and S. Cui, "Optimal power allocation for outage probability minimization in fading channels with energy harvesting constraints," *IEEE Transactions on Wireless Communications*, vol. 13, no. 2, pp. 1074–1087, 2014.
- [41] S. Wei, W. Guan, and K. R. Liu, "Power scheduling for energy harvesting wireless communications with battery capacity constraint," *IEEE Transactions on Wireless Communications*, vol. 14, no. 8, pp. 4640–4653, 2015.

- [42] G. Ardeshiri and A. Vosoughi, "Learning-based distributed detection with energy harvesting," in 2021 55th Asilomar Conference on Signals, Systems, and Computers, 2021, pp. 747–751.
- Systems, and Computers, 2021, pp. 747–751.
 [43] M. Kashef and A. Ephremides, "Optimal packet scheduling for energy harvesting sources on time varying wireless channels," *Journal of Communications and Networks*, vol. 14, no. 2, pp. 121–129, 2012.
- [44] M. Salehi Heydar Abad, O. Ercetin, and D. Gündüz, "Channel sensing and communication over a time-correlated channel with an energy harvesting transmitter," *IEEE Transactions on Green Communications* and Networking, vol. 2, no. 1, pp. 114–126, 2018.
- [45] H. Liu, X. Zhao, H. Liang, and Z. Li, "Pomdp-based energy cooperative transmission policy for multiple access model powered by energy harvesting," *IEEE Transactions on Vehicular Technology*, vol. 68, no. 6, pp. 5747–5757, 2019.
- [46] W. Li, M.-L. Ku, Y. Chen, and K. R. Liu, "On outage probability for stochastic energy harvesting communications in fading channels," *IEEE Signal Processing Letters*, vol. 22, no. 11, pp. 1893–1897, 2015.
- [47] F. Zhang, T. Jing, Y. Huo, and K. Jiang, "Joint Optimization of Spectrum Sensing and Transmit Power in Energy Harvesting Cognitive Radio Sensor Networks," *The Computer Journal*, vol. 62, no. 2, pp. 215–230, 02 2019.
- [48] H.-K. Chang, M.-L. Ku, and J.-C. Lin, "On stochastic link and energy scheduling for energy harvesting bidirectional communications," *IEEE Access*, vol. 8, pp. 20129–20145, 2020.
- [49] W. Li, M.-L. Ku, Y. Chen, K. R. Liu, and S. Zhu, "Performance analysis for two-way network-coded dual-relay networks with stochastic energy harvesting," *IEEE Transactions on Wireless Communications*, vol. 16, no. 9, pp. 5747–5761, 2017.
- [50] R. Ma and W. Zhang, "Optimal power allocation for energy harvesting communications with limited channel feedback," in 2014 IEEE Global Conference on Signal and Information Processing (GlobalSIP). IEEE, 2014, pp. 193–197.
- [51] Q. Li, J. Gao, H. Liang, L. Zhao, and X. Tang, "Optimal power allocation for wireless sensor powered by dedicated rf energy source," *IEEE Transactions on Vehicular Technology*, vol. 68, no. 3, pp. 2791–2801, 2019.
- [52] X. Guo, Y. He, S. Atapattu, S. Dey, and J. S. Evans, "Power allocation for distributed detection systems in wireless sensor networks with limited fusion center feedback," *IEEE Transactions on Communications*, vol. 66, no. 10, pp. 4753–4766, Oct 2018.
- [53] S. Mao, M. H. Cheung, and V. W. S. Wong, "Joint energy allocation for sensing and transmission in rechargeable wireless sensor networks," *IEEE Transactions on Vehicular Technology*, vol. 63, no. 6, pp. 2862– 2875, July 2014.
- [54] M. Ku, Y. Chen, and K. J. R. Liu, "Data-driven stochastic models and policies for energy harvesting sensor communications," *IEEE Journal* on Selected Areas in Communications, vol. 33, no. 8, pp. 1505–1520, Aug 2015.
- [55] J.-J. Xiao, S. Cui, Z.-Q. Luo, and A. J. Goldsmith, "Power scheduling of universal decentralized estimation in sensor networks," *IEEE Trans*actions on Signal Processing, vol. 54, no. 2, pp. 413–422, 2006.
- [56] A. Sani and A. Vosoughi, "Distributed vector estimation for power-and bandwidth-constrained wireless sensor networks," *IEEE Transactions on Signal Processing*, vol. 64, no. 15, pp. 3879–3894, 2016.
- [57] M. L. Puterman, Markov decision processes: discrete stochastic dynamic programming. John Wiley & Sons, 2014.
- [58] M. Moghadari, E. Hossain, and L. B. Le, "Delay-optimal distributed scheduling in multi-user multi-relay cellular wireless networks," *IEEE Transactions on Communications*, vol. 61, no. 4, pp. 1349–1360, April 2013
- [59] F. Fu and M. V. Der Schaar, "A systematic framework for dynamically optimizing multi-user wireless video transmission," *IEEE Journal on Selected Areas in Communications*, vol. 28, no. 3, pp. 308–320, April 2010.
- [60] D. Bertsekas, Dynamic programming and optimal control: Volume I. Athena scientific, 2012, vol. 1.
- [61] D. G. Luenberger and Y. Ye, *Linear and nonlinear programming*, 4th ed. Springer, 2015.
- [62] N. Maleki, A. Vosoughi, and N. Rahnavard, "Distributed binary detection over fading channels: Cooperative and parallel architectures," *IEEE Transactions on Vehicular Technology*, vol. 65, no. 9, pp. 7090–7109, 2015.
- [63] R. Niu and P. K. Varshney, "Target location estimation in sensor networks with quantized data," *IEEE Transactions on Signal Processing*, vol. 54, no. 12, pp. 4519–4528, 2006.



Ghazaleh Ardeshiri received the B.Sc. degree in 2012 and the M.Sc. degree in 2017 both in electrical engineering from Shiraz University, Shiraz, Iran. She is currently working toward her Ph.D. in electrical engineering at the University of Central Florida. Ms. Ardeshiri's current research interests include distributed detection, statistical signal processing and energy harvesting in wireless sensor networks.



Azadeh Vosoughi (M'06, SM'14) is an Associate Professor in the Department of Electrical and Computer Engineering at the University of Central Florida. She received her B.S. degree from Sharif University of Technology, Tehran, Iran, in 1997; her MS degree from Worcester Polytechnic Institute, Worcester, MA, in 2001; and her Ph.D. degree from Cornell University, Ithaca, NY, in 2006, all in Electrical Engineering. Her research interests lie in the general areas of wireless communications, statistical signal processing, distributed detection and

tistical signal processing, distributed detection and estimation theory, and brain signal processing. Dr. Vosoughi received the NSF CAREER award in 2011.